

**MEMS BIOSENSOR FOR DETECTION OF *ESCHERICHIA*  
*COLI O157:H7* IN FOOD PRODUCTS**

---

A Thesis  
presented to  
the Faculty of the Graduate School  
at the University of Missouri-Columbia

---

In Partial Fulfillment  
of the Requirements for the Degree  
Master of Science

---

By  
**SHIBAJYOTI GHOSH DASTIDER**  
Dr. Mahmoud Almasri, Thesis Supervisor

JULY 2011

The undersigned, appointed by the dean of the Graduate School, have examined the thesis entitled

MEMS BIOSENSOR FOR DETECTION OF *ESCHERICHIA COLI O157:H7* IN FOOD PRODUCTS

presented by Shibajyoti Ghosh Dastider

a candidate for the degree of Master of Science,

and hereby certify that, in their opinion, it is worthy of acceptance.

---

Dr. Mahmoud Almasri

---

Dr. Zaichun "Frank" Feng

---

Dr. Naz Islam

## ACKNOWLEDGEMENTS

*“There is no such thing as a self-made man. You will reach your goals only with the help of others.”* Similar to this quote this thesis would not have been possible without the encouragement, guidance and help of several individuals who in one way or another contributed in my research and made this a reality.

First, I would like to express my heartily gratitude towards my advisor Dr. Mahmoud Almasri for providing me the opportunity to work with him and be part of the Microsystem Research Laboratory. I would like to thank him for his continuous encouragement, guidance, support and help throughout these years. I am grateful to Dr. Majed El-Dweik for letting me use the Nanotechnology Center at Lincoln University and providing me with all necessary things, required for the biological part of my research.

I would also like to express my sincere thanks to all my committee members Dr. Mahmoud Almasri, Dr. Zaichun "Frank" Feng and Dr. Naz Islam for taking their time to read my thesis and contributing with their valuable suggestions towards completion of this work.

I thank the friendly and cheerful group of fellow students for their help and support during my research. I am also thankful to Ms. Shirley Holdmeier for always helping me with my official works.

I am grateful to my parents and my elder sister for whatever I am today. Their contribution in my life is invaluable. Along with them, I would like to thank my brother-in-law for being a great friend, philosopher and guide. I also thank all my friends and family members for their love and support.

## TABLE OF CONTENTS

ACKNOWLEDGEMENTS .....	II
LIST OF FIGURES .....	V
LIST OF TABLES .....	VII
ABSTRACT .....	VIII
CHAPTER 1: Introduction .....	1
1.1 Overview of MEMS and BioMEMS Applications .....	1
1.1.1 Biosensors .....	2
1.2 Motivation and Significance .....	8
1.3 Outline of the Thesis .....	9
CHAPTER 2: Theoretical Background .....	11
2.1 Impedance Biosensor Equivalent Circuit .....	11
2.1.1 Equivalent Circuit Model .....	12
2.2 Dielectrophoresis for Cell Separation .....	15
2.3 Bacteria Detection Mechanism: Impedance Spectroscopy .....	19
CHAPTER 3: Design and Modeling .....	20
3.1 Biosensor Design .....	20
3.1.1 Biosensor Design-I .....	21
3.1.2 Biosensor Design-II .....	22
3.2 Layout Designing Using CAD Tools .....	24
3.3 Electric Field Modeling .....	29
CHAPTER 4: Fabrication of Biosensor .....	31
4.1 Materials Used in the Fabrication .....	31
4.1.1 Glass Slide .....	31
4.1.2 Metals .....	32
4.1.3 Polydimethylsiloxane (PDMS) .....	33
4.2 Fabrication .....	34
4.2.1 Surface Purification of Glass Slide .....	35
4.2.2 Deposition of Metals .....	35
4.2.3 Photolithography .....	37
4.2.4 Patterning Interdigitated Electrode Arrays, Traces and Bonding Pads .....	38

4.2.5 Creating PDMS Microchannel Block .....	41
4.2.6 Creating Top PDMS-Fluidics Connector Block .....	43
4.2.7 Bonding PDMS to Glass.....	45
4.2.8 Wire Bonding and Packaging .....	46
CHAPTER 5: Test Setup and Protocol.....	47
5.1 Test Setup.....	47
5.1.1 Fluid Flow in the Channel .....	48
5.1.2 Agilent 4294A Precision Impedance Analyzer .....	48
5.1.3 Lecia DM-IL Inverted Contrasting Microscope .....	49
5.2 Chemical and Reagents.....	50
5.3 Bacteria Culture .....	51
5.4 Surface Modification and Immobilization of <i>E.coli</i> Cells.....	52
CHAPTER 6: Results and Discussion .....	54
6.1 Impedance Measurement and Analysis .....	54
6.2 Sensitivity Measurement.....	55
6.3 Test of Sensitivity towards Non- <i>E.coli</i> Bacteria.....	62
6.4 Real-Time Measurement and Detection .....	64
CHAPTER 7: Conclusion and Future Work.....	65
7.1 MEMS Based Impedance Biosensor for <i>E.coli O157:H7</i> Detection.....	65
7.2 The Study of Sensitivity.....	66
7.3 Scope of Commercialization.....	67
7.4 Future Work.....	68
REFERENCES .....	69

## LIST OF FIGURES

Figure 1.1. Interdigitated Electrode Array .....	4
Figure 1.2 Interdigitated Array Microelectrode Immunosensor by Yang, L. Et Al. ....	4
Figure 1.3 Microimpedance Biosensor For Bacterial Detection by Radke, Alocilja. ....	5
Figure 1.4 Double Idm-Based Impedance Biosensor by Madhukar Varshneya et al.....	6
Figure 2.1 Electrical Equivalent Circuit of a Cell.....	12
Figure 2.2 Electrical Equivalent Circuit (Using Eis) .....	13
Figure 2.3 Dipole Movement (Equal And Opposite Dipoles). ....	15
Figure 2.4 Dipole Movement (Unequal And Opposite Dipoles).....	16
Figure 2.5 Schematic Diagram Showing the Positive and Negative Dielectrophoretic forces on particles subjected to non-uniform electric fields. ....	17
Figure 3.1 Biosensor Design – I .....	22
Figure 3.2 Biosensor Design – II .....	23
Figure 3.3 Biosensor Design – I Layouts a) Magnified View of Interdigitated Microelectrode b) Microchannel c) Design – I Entire Layout.....	25
Figure 3.4 Biosensor Design – II Layouts a) Interdigitated Microelectrodes B) Magnified View of Interdigitated Microelectrode c) Microchannel .....	27
Figure 3.5 a) Focusing Ida With Microchannel b) Complete Layout of Design – II .....	28
Figure 3.6 Electric Field Distribution Across Focusing Electrode Array A) Three Dimensional View, a) Cross Section View.....	29
Figure 3.7 Electric Field Distribution Across Focusing Electrode Array a) Three Dimensional View, b) Cross Section View. ....	29
Figure 4.1 Crosssectional view of fabrication process .....	34
Figure 4.2 Piranha cleaned Glass slide .....	35
Figure 4.3 A) Sputtering system B) Graphical illustration Of Sputtering .....	36
Figure 4.4 Glass slide sputtered with Cr And Au .....	37
Figure 4.5 Spincoater used for photoresist coating.....	38
Figure 4.6 Maskaligner used for photolithography.....	39
Figure 4.7 Interdigitated Gold Microelectrodes under optical microscope .....	40

Figure 4.8 SEM image of the Interdigitated Gold Microelectrodes .....	40
Figure 4.9 20x Magnified view of Gold Interdigitated Microelectrodes .....	41
Figure 4.10 SEM Images of the Microchannel SU-8 mold on Si substrate.....	42
Figure 4.11 Si Substrate with SU-8 Microchannel mold.....	43
Figure 4.12 SEM Images of the inlet and outlet of the Microchannel on PDMS.....	44
Figure 4.13 Cured PDMS slabs with Microchannel and Microfluidics Connectors .....	44
Figure 4.14 Plasmalab 80 (Reactive Ion Etching Tool) used to bond PDMS to Glass ....	45
Figure 4.15 Fabricated Device.....	46
Figure 4.16 Packaged Biosensor.....	46
Figure 5.1 Graphical illustration of the Test Setup.....	48
Figure 5.2 Setup with Impedance Analyzer.....	49
Figure 5.3 Biosensor under microscope for Optical Observation.....	50
Figure 5.4 Centrifuged Test solution .....	51
Figure 5.5 Immobilization Process .....	53
Figure 6.1 Impedance Spectroscopy using Impedance Analyzer .....	55
Figure 6.2 Magnified view of four concentrations of <i>E. Coli O157:H7</i> cells on Interdigitated Electrodes .....	56
Figure 6.3 Impedance Responses of four different concentrations of <i>E.Coli O157:H7</i> in Grape Sample.....	57
Figure 6.4 Impedance responses of four different concentrations of <i>E.Coli O157:H7</i> in Spinach Sample.....	58
Figure 6.5 Impedance responses of four different concentrations of <i>E.Coli O157:H7</i> in Turkey Sample .....	59
Figure 6.6 Impedance responses of <i>Salmonella Typhimurium</i> samples in Grape Medium .....	62

## LIST OF TABLES

Table 6-1 Various concentrations and the test medium used for impedance measurement .....	54
Table 6-2 Impedance values of four samples at nine frequency points from 100Hz to 1MHz .....	61
Table 6-3 Impedance values of four samples at nine frequency points from 100Hz to 1MHz .....	61
Table 6-4 Impedance values of four samples at nine frequency points from 100Hz to 1MHz .....	61
Table 6-5 Impedance values of four samples at nine frequency points from 100Hz to 1MHz .....	63



## ABSTRACT

*Escherichia coli* O157:H7, a gram-positive bacterium, is one of the most common pathogens and causes several *E.coli* infection outbreaks throughout the year. *E. coli* infection results in severe illness such as diarrhea, urinary tract infections, respiratory illness, pneumonia, etc. Every year in the United States, thousands of people fall victim to *E.coli* infection and many are hospitalized. In the last five years there have been at least 12 outbreaks of *E.coli* on various farms, ranches and dairies across the country. In 2010-11 there were 5 outbreaks of *E.coli* in food products such as beef, romaine lettuce, cheeses, hazelnuts and *Lebanon bologna products*. Thus there is an immediate need for sensors capable of rapid detection of pathogenic strains of *E.coli* in food products to reduce the amount of infection and outbreaks.

To effectively detect the presence of *E.coli* O157:H7 in food products a MEMS based biosensor has been designed and fabricated. This MEMS biosensor detects the *E.coli* bacteria based on the principal of impedance spectroscopy. The biosensor consists of planar interdigitated array of microelectrodes (IDAM) and a microchannel. The surface of the microelectrodes is modified using goat *anti-E.coli polyclonal IgG* antibody. As the *E.coli* sample is injected inside the biosensor through the microchannel, it comes in contact with the modified electrode surface. As soon as the *E.coli* bacterium cells get recognized by the *anti-E.coli* antibody it binds to the antibody. This binding changes the dielectric property of the electrodes, and as a result, the impedance of the device changes. The change in impedance is measured using an impedance analyzer

which allows the study of the impedance response of the biosensor for a frequency range of 100 Hz - 1MHz.

Another variation of this biosensor has been designed and proposed in this thesis. This design consists of two arrays of 3-dimensional electrodes and a microchannel with multiple inlets and outlets. In this design the first array of interdigitated electrodes is used to separate unwanted objects from the sample using dielectrophoresis. The second array of 3-dimensional microelectrodes acts as a detection array and its surface is modified in similar fashion using *anti-E.coli* antibody. When the clean sample with *E.coli cells* reach the detection array, the bacteria cells get immobilized on the electrode surface causing a change in the dielectric property.

To investigate the sensitivity and selectivity of the biosensor, the impedance response is studied for various *E.coli* samples. From the analysis of the obtained response it was found that the lower detection limit of the biosensor is  $3 \times 10^3$  CFU/ml and it is sensitive to various concentrations of *E.coli* samples. This means the developed biosensor can detect as low as 3 cells/ $\mu$ l. The biosensor was also tested for its selectivity and it was observed that it is only responsive to *E.coli O157:H7* bacterium cells. The selectivity of the biosensor can be altered by changing the type of antibody immobilized on the sensor surface. Thus it can be used for detecting other types of pathogens too. The clinical detection time for *E.coli* bacteria using Colilert / Colitag methods (Enumeration) can take up to 24 hours. But the total detection time for this biosensor is about 30 minutes which is rapid compared to the conventional ways of detection. Also as the biosensor is small and portable, it can accommodate onsite testing, and owners of farms, dairies and ranches wouldn't have to send their produce and/or meat products to a laboratory for

sampling and pathogenic tests. All these features including optimal sensitivity, selectivity, fast response time and rapid detection ability give this biosensor great potential for industrial and societal benefit through implementation.

## CHAPTER 1: **Introduction**

This chapter provides overview of microelectromechanical systems (MEMS) and biomedical MEMS (BioMEMS) applications in many fields. Different MEMS based biosensors for detection of pathogens are discussed and compared. A general outline of the thesis is also presented.

### **1.1 Overview of MEMS and BioMEMS Applications**

Miniaturization of electrical circuits and systems has resulted in a technological revolution responsible for hundreds of billions of dollars spent in the integrated-circuit (IC) industry. The advent of IC has changed the world economy and improved the way we live and work [1,2].The field of microelectromechanical systems (MEMS) represents ways to improve the scale and performance of these systems as well as reduce their size and cost. This is achieved by employing batch-fabrication and the large scale manufacturing techniques successfully incorporated by the IC industry [3]. Interest in development of MEMS has seen a huge growth during the past decade. MEMS use well-established IC-based microfabrication techniques to make integrated circuits. MEMS devices have already achieved huge success in a number of commercial applications such as projection displays and in the measurement of pressure and acceleration. New applications continue to emerge as MEMS technology is applied to the miniaturization

and integration of various systems [4]. MEMS's rapid growth in the last two decades has reached beyond the early electrical or mechanical systems and are now widely used in other domains such as, physics, chemistry, biology, medicine, aerospace optics, etc. [5].

Biomedical Microelectromechanical Systems (BioMEMS), a subset of MEMS, has emerged, with a growing number of applications of MEMS devices in the Biomedical field [6]. Areas of research and applications of BioMEMS include (but not limited to) diagnostics of biological cells, DNA and protein micro-array analysis, novel bio-compatible materials, micro-fluidics, tissue engineering, surface modification, implantable BioMEMS systems, and Smart drug delivery systems [7].

### **1.1.1 Biosensors**

Biosensors are analytical devices composed of a biological recognition element(s) and a physical or chemical transducer(s) to selectively and quantitatively detect the presence of specific compounds in a given external environment. The transducer converts the change in the property of the solution, surface, etc. to a recordable signal level [8]. During the last decade, various kinds of MEMS biosensors were fabricated and manufactured which allowed sensitive, rapid, and real-time detection of cells, proteins, DNA, or small molecules [9, 10]. Many of these are based on a single element. These single elements can be serially combined together to create an array of biosensors. Depending on the application, the detection method of the biosensor varies. A few popular detection methods used for MEMS based biosensors include electromechanical, electrical, and optical detection [7]. There are various kinds of electrochemical biosensors, such as amperometric, potentiometric, conductimetric, or impedimetric.

These electrochemical biosensors are advantageous as they are highly sensitive, have rapid sense time, low manufacturing cost, and can be combined with other systems to create an integrated microsystems [11, 12]. These sensors measure the electrochemical impedance which combines the analysis of resistive, capacitive or inductive properties of materials. [13, 14].

Electrochemical impedance biosensors detect the target molecules by measuring the change in impedance. The target molecule binds to the receptors such as, antibodies, DNA, proteins or other bio-recognition elements which are immobilized on the surface of the electrodes [15, 11, 16, 17]. The impedance change may result due to the change in conductivity of the medium caused by the growth of bacteria [18, 19, 15, 20], due to suspension of target molecules in the aqueous medium [21, 22], entrapment of bacterial cells on the surface of electrodes using dielectrophoresis (DEP) [23, 24, 25, 26, 27], and change in the ionic concentration of the medium caused by the activity of enzymes (used as labels for the signal amplification) [28, 29, 30, 31]. In some early electrochemical impedance biosensors, large metal rods or wires were used as electrodes to measure impedance [32, 33, 34]. To improve the sensitivity and miniaturize the size of the sensor system the potential of microelectrode based sensor systems were considered and combined with traditional detection system [35].

Among microelectrodes, interdigitated microelectrode arrays (IDAM) are most popular. IDAM has some considerable advantages over other type of electrode systems. It has low ohmic drop, fast establishment of steady-state and also rapid reaction kinetics [36, 37]. The increased signal-to-noise ratio and the low response time also provides rapid detection using IEA [35, 38]. Moreover IDAM has a significant advantage over

three or four electrode system as this detection system doesn't require a reference electrode and provides simple means to obtain steady-state response [39, 40]. IDAM consist of a series of parallel electrodes forming two comb shapes. The two electrodes are connected together forming an array of interdigitated electrodes. A 3-dimensional picture of the interdigitated microelectrode array is shown in Figure. 1.1.

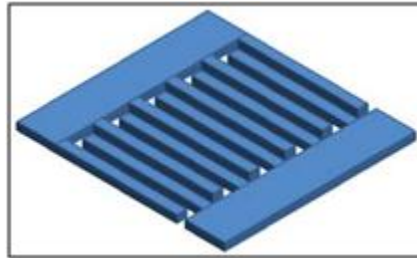


**Figure 1.1. Interdigitated Electrode Array**

Several devices for detecting biological cells using the impedimetric detection principle have been fabricated and tested. Yang, L. et al. designed an interdigitated microelectrode array based electrochemical impedance immunosensor for detection of *Escherichia-coli O157:H7* (see Figure 1.2) [15].

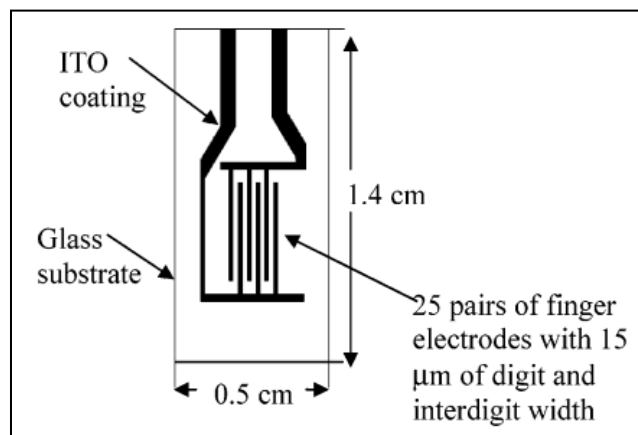


**Figure 1.2 Interdigitated Array Microelectrode Immunosensor by Yang, L. et al. [15].**

The interdigitated electrode array was constructed of indium-tin oxide. The array was coated with *E.-coli* antibody. The immobilization of antibodies and the formation of

antibody cell complexes on the surface of the IDA microelectrode were characterized by cyclic voltammetry and two-electrode Faradaic electrochemical impedance spectroscopy in the presence of  $[\text{Fe}(\text{CN})_6]^{3/4}$  as a redox probe [15]. Electron-transfer resistance of the electrode increased upon the immobilization of the antibody and the binding of *E-coli* cells [15]. The electron-transfer resistance was correlated with the concentration of *E-coli* cells in a range from  $4.36 \times 10^5$  to  $4.36 \times 10^8$  cfu/mL with the detection limit of  $10^6$  cfu/mL. G. Kim et al. [41] proposed an interdigitated microelectrode based impedance biosensor for detection of *Salmonella Enteritidis* in food samples. The Interdigitated microelectrode (IME) sensor was fabricated from a glass wafer with a 50 nm Cr layer as an adhesive layer [41]. A 100 nm thick of interdigitated gold electrode was deposited over the Cr layer and patterned using photolithographic processing methods to form an active sensing

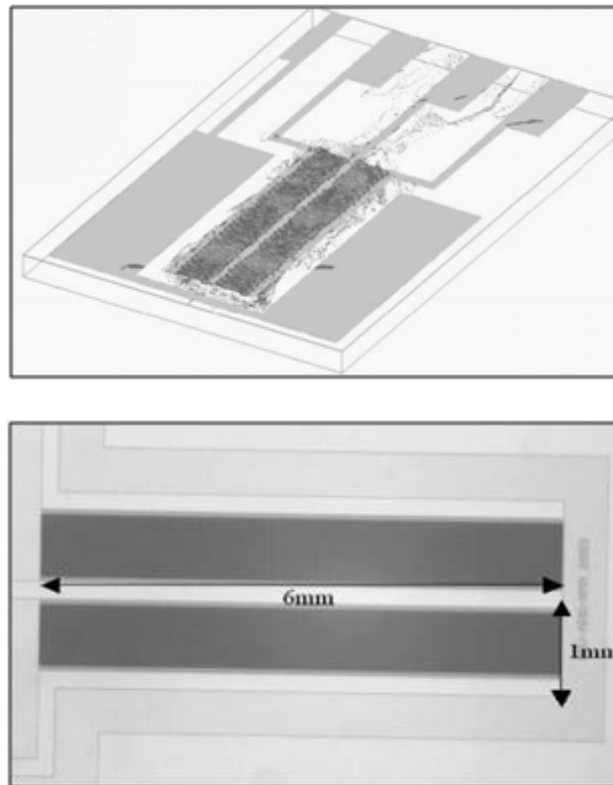


**Figure 1.3 Microimpedance Biosensor for Bacterial Detection by Radke, Alocilja [16].**



area [41]. Three different sensor types, each with different electrode gap sizes (2  $\mu\text{m}$ , 5  $\mu\text{m}$ , 10  $\mu\text{m}$ ), were fabricated to evaluate the effect of electrode specification on the sensitivity. Radke, S.M. and Alocilja[16] developed an impedance biosensor for bacterial detection, which can discriminate between different cellular concentrations from  $10^5$  to  $10^7$  CFU/mL in pure culture (See Figure 1.3). The sensor detected the change in impedance caused by the presence of bacteria immobilized on interdigitated gold electrodes and was fabricated from (100) silicon with a 2  $\mu\text{m}$  layer of thermal oxide as an insulating layer [16].

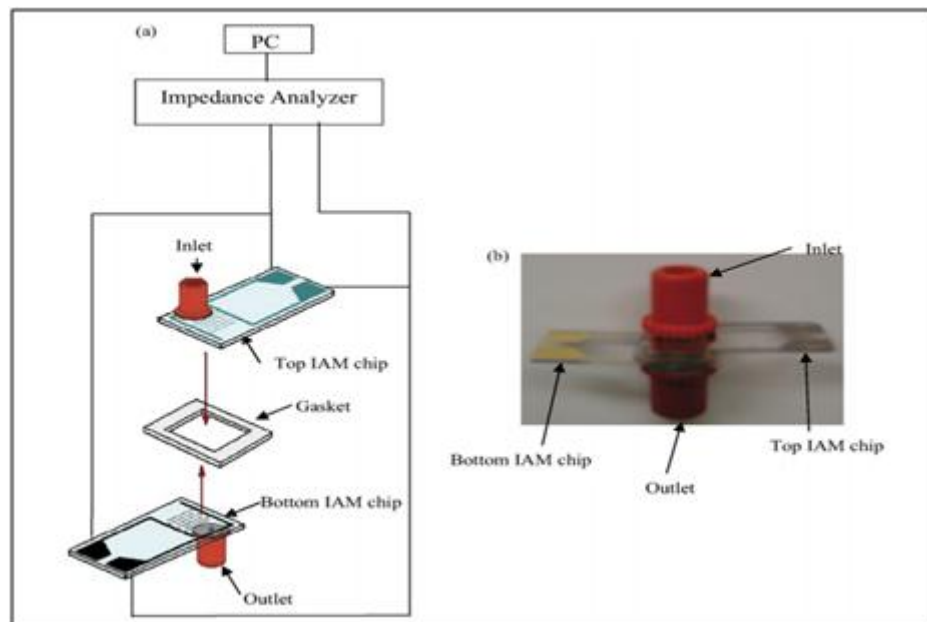


**Figure 1.4 Double IDM-based impedance biosensor by Madhukar Varshneya et al. [35].**

The sensor active area is  $9.6 \text{ mm}^2$  and consists of two interdigital gold electrode arrays measuring  $0.8 \times 6 \text{ mm}$  [16]. The surface was coated with *E-coli* specific antibody between the electrodes to create a biological sensing surface [16]. The impedance across the interdigitated electrodes was measured after immersing the biosensor in solution. Bacteria cells present in the sample solution attached to the antibodies and became

tethered to the electrode array, thereby causing a change in measured impedance [16]. Madhukar Varshneya and Yanbin Li fabricated double Interdigitated Array Microelectrode (IAM) based impedance biosensor to detect *E-coli* O157:H7 after enrichment in growth medium (See Figure 1.4) [35]. This study was aimed at the design of a simple flow cell with an embedded IAM which does not require complex microfabrication techniques and can be used repeatedly with a simple assembly/disassembly step [35].

The flow cell was also unique in having two IAM chips on both top and bottom surfaces of the flow cell, which enhances the sensitivity of the impedance measurement [35]. The impedance biosensor successfully detected *E-coli* O157:H7 in a range from 8.0 to  $8.2 \times 10^8$  CFUmL<sup>-1</sup> after an enrichment growth of 14.7 and 0.8 h, respectively [35]. Binu Baby Narakathue et al. designed and fabricated an impedance based electrochemical biosensor for the detection of various chemical and biological species [42]. The device is a flow cell with inlet and outlet ports, built on a glass substrate with gold electrodes (See Figure 1.5).

The flow cell was fabricated using acrylic material with a reservoir volume of 78  $\mu$ l. The impedance based response of the two-terminal device revealed a very high sensitivity with low concentrations of Potassium Chloride (KCl), Cadmium Sulphide (CdS), Mouse Monoclonal IgG, and D - Proline at pico mole levels [42].

## 1.2 Motivation and Significance

*Escherichia coli* (abbreviated as *E. coli*) are Gram-negative rod-shaped bacterium. Although most strains of *E. coli* are harmless, some can cause diarrhea, while others cause urinary tract infections, respiratory illness and pneumonia, and other illnesses. In 2010-11 *E. coli* O157:H7 outbreaks in the United States were associated with beef from National Steak and Poultry and Dutch Style Goudacheese from Bravo Farms. In addition, a multistate outbreak of *E. coli* O157:H7 infection was associated with in-shell hazelnuts distributed by DeFranco and Sons of Los Angeles, CA, and another multistate outbreak of *E. coli* O157:H7 infection was associated with Seltzer's Beef Lebanon Bologna distributed by Palmyra Bolgna Co. in Palmyra, PA. *E. coli* O157:H7 is clearly one of the deadliest food borne pathogenic bacteria. It causes an estimated 73,000 cases of infection and 61 human deaths in the United States each year (Centers for Disease Control and Prevention, 2006). This bacterium has been linked to hemolytic uremic syndrome and hemorrhagic colitis. These illnesses may cause diarrhea, seizure, stroke, kidney failure and even death (Food and Drug Administration, 2008). They are often misdiagnosed, resulting in expensive medical testing before they are correctly diagnosed. In addition, *E. coli* has the potential to cause enormous national and international economic devastation due to medical costs and product recalls. It can also be found in vegetables, unpasteurized milk, juice and unchlorinated water. Contamination can have a significant impact on businesses such as the beef -industry. *E. coli* O157:H7 can be found on most cattle farms and can live in the intestines of healthy cattle. Thus, the meat can become contaminated with *E. coli* O157:H7 during slaughter. It is important to note that the infectious doses of

*E. coli* O157:H7 is as low as 10 cells (Federal Register, 1990, 1991). Therefore, effective detection techniques are crucial to monitor and control *E. coli* O157:H7 in food products.

Testing for the bacteria requires extensive analysis which has to meet certain challenging criteria. Sensitivity and response time for the analysis are imperative factors related to the usefulness of microbiological testing. An extremely selective detection methodology is also required because low numbers of pathogenic bacteria are often present in a complex biological environment along with many other nonpathogenic organisms. Traditional methods for the detection of bacteria cannot meet the deadline desired in a clinical laboratory. In response to this problem, a number of instruments have been developed using various principles of detection, such as flow cytometry polymerase chain reaction, immunomagnetic separations, bioluminescence and mass spectrometry. These conventional methods for detection and identification involve prolonged multiple enrichment steps; thus, are time consuming and expensive.

To overcome these problems and to provide better detection technology in a simple, portable, and low-cost system, the research featured in this thesis has developed two designs for an impedemetric biosensor, here after referred to as an impedance biosensor.

### **1.3 Outline of the Thesis**

In this thesis an interdigitated microelectrode array (IDE) based impedance biosensor is defined with all of its applications and potential presented for consideration. The biosensor has two different designs. The first design uses a single 2-D array of Interdigitated Micro Electrodes (IME) whereas the second design has a 3-D array of IME. The IME is covered with a micro channel through which the bacteria medium is flown.

IME measures the change in impedance when the antibody and antibody-cell complexes are immobilized on the surface. The main advantage of the 3-D biosensor is the increased surface area to volume ratio compared to other electrochemical sensors. This will enhance the sensitivity of impedance detection and its capability to confine few live bacterial cells in nano liters volume which can then be microchanneled for rapid detection and identification of *E.coli bacteria*.

The first chapter of this thesis provides introduction to various MEMS and BioMEMS technologies. It also provides information about different MEMS based electrochemical devices and Biosensors. The second chapter explains the motivation, purpose of this work and the theoretical background. The equivalent circuit of the biosensor and the effect of dielectrophoresis on detection will also be discussed here. The third chapter discusses the design, modeling and simulation of the biosensor. Chapter four describes the fabrication process of the biosensor in detail. Chapter five describes the experimental setup, equipments and the biological aspect of the testing. The process of culturing cells, incubation and detection of bacteria is also described in details. The obtained results and the analysis of the results are discussed in chapter six. Finally, the conclusion of the thesis work is summarized in chapter seven.

## CHAPTER 2: **Theoretical Background**

This chapter explains the theoretical aspects of the impedance biosensor. Equivalent circuit for the biosensor is defined followed by a discussion of the impedance sensing mechanism. Dielectrophoresis which is used to focus the bacteria into the center of the channel is also discussed.

### **2.1 Impedance Biosensor Equivalent Circuit**

Impedance of the biosensor can't be directly calculated as the distribution of current through the test sample (electrolyte) is non-uniform, which creates difficulty in determining the correct path of current flow. Thus the equivalent circuit plays an important role in understanding the response of the biosensor. The equivalent circuit consists of the electrical parameters responsible for the impedance change. The electrical parameters generally used to design an equivalent circuit model include electrolyte resistance (bulk medium resistance), double layer capacitance, dielectric capacitor, etc. The types of electrical components in the model and their interconnections control the shape of the equivalent circuit's impedance spectrum, and the circuit parameters control the size of each feature in the spectrum.

### 2.1.1 Equivalent Circuit Model

The equivalent circuit model for the biosensor is shown in Figure 2.1. The equivalent circuit consists of two parallel branches. Each branch consists of different components representing a specific chemical process taking place in the biosensor. The test solution and electrolyte present in-between the electrodes contribute a resistive element to the equivalent circuit. This is represented as resistance of the solution ( $R_{sol}$ ). The cells present in-between the electrodes also generate impedance ( $Z_{cell}$ ).

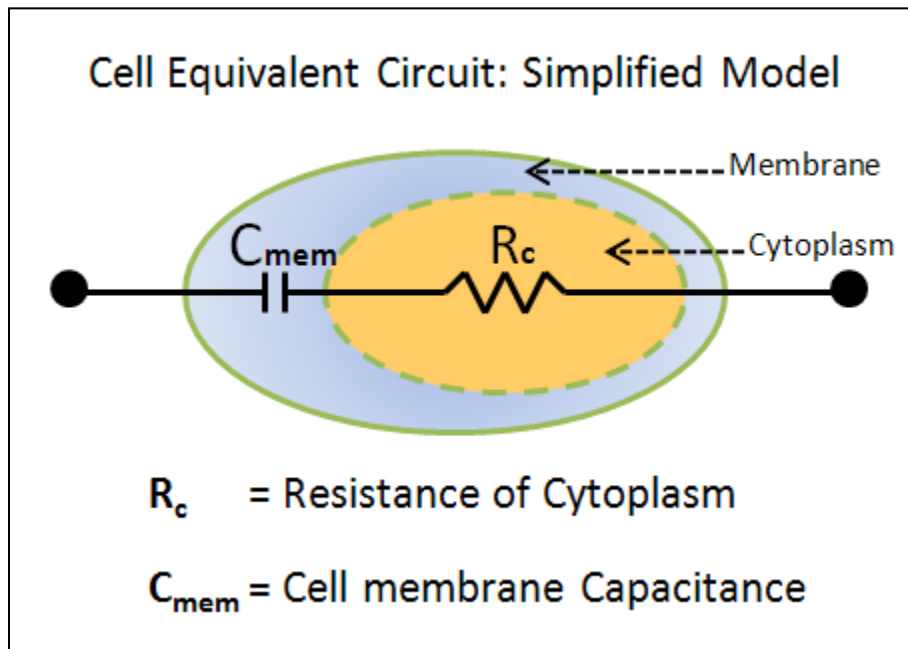


Figure 2.1 Electrical Equivalent Circuit of a Cell [43]

It consists of cell membrane and various components which are suspended in the cytoplasm. As the cell membrane has a very high resistance compared to the reactance, the resistance is ignored. So the cell membrane acts as a capacitor. On the other hand, cytoplasm's reactance is ignored when compared to its resistance and it behaves like a resistor. Thus the impedance of the cell can be described as a series combination of capacitor and resistor [43]. When two electrode surfaces are separated and have an

electrolyte substance between them, a thin layer of charged particles is created on the surface of the electrodes. When two electrode surfaces are separated and have an electrolyte substance between them, a thin layer of charged particles is created on the surface of the electrodes.

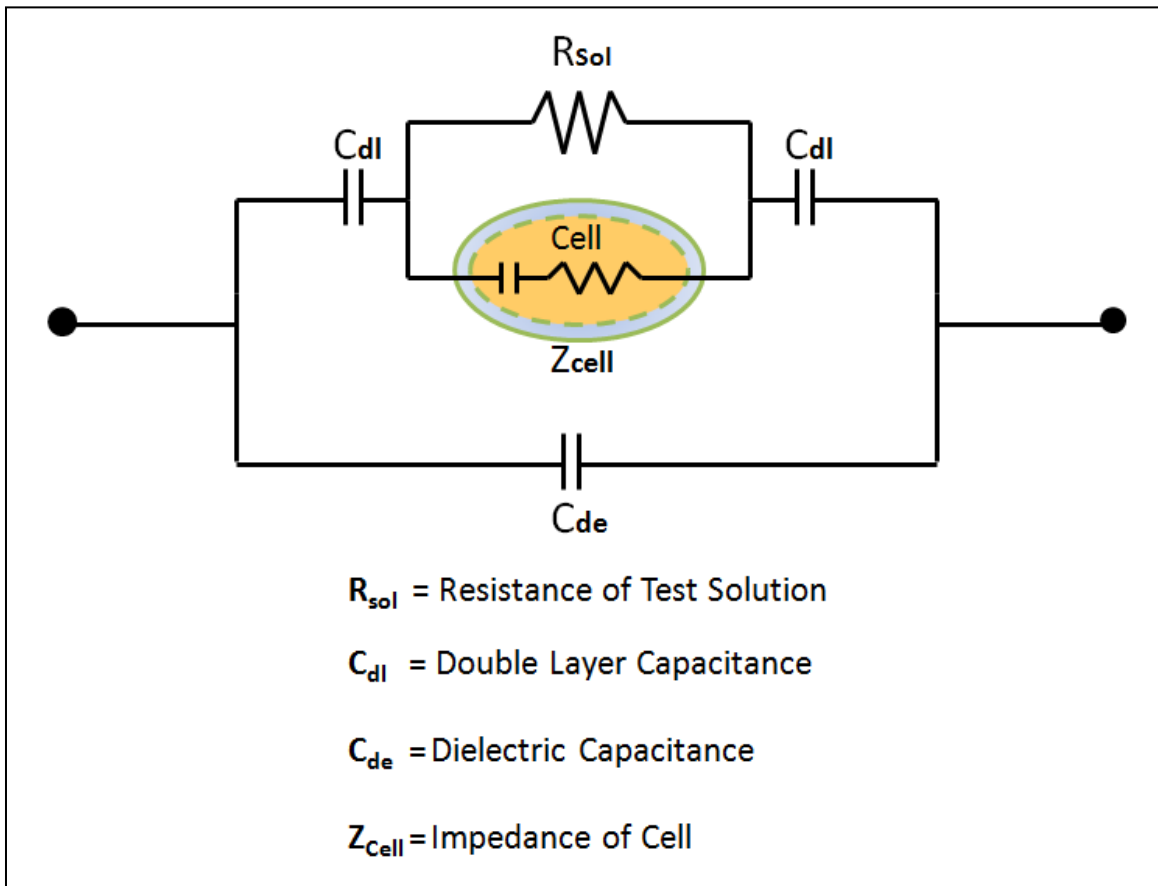


Figure 2.2 Electrical Equivalent Circuit (using EIS) [21]

This thin layer of charged particles generates a capacitance, called double layer capacitance ( $C_{dl}$ ). Thus, the interface between the electrodes and the test solution (electrolyte) exhibits impedance ( $Z_{dl}$ ), which depends on the double layer capacitance  $C_{dl}$ . Double layer capacitance is typically in the nanofarads (nF) range. The dielectric capacitance ( $C_{de}$ ) counts for the overall capacitance of the dielectric medium present and the stray capacitance of the impedance measurement system.



The total impedance of each branch is indicated as  $Z_1$  and  $Z_2$  given by the expressions,

$$|Z_1| = \sqrt{(R_{sol} || Z_{cell})^2 + \frac{1}{(\pi f C_{dl})^2}} \quad (1)$$

$$|Z_2| = \sqrt{\frac{1}{(2\pi f C_{de})^2}} \quad (2)$$

The Magnitude of Total Impedance ( $|Z|$ ) is given by the expression,

$$|Z| = \frac{Z_1 * Z_2}{Z_1 + Z_2} \quad (3)$$

At low frequencies, current cannot pass through  $C_{de}$  and acts as open circuit. Thus at low frequencies only  $C_{dl}$ ,  $R_{sol}$   $Z_{cell}$  is responsible for the impedance response of the biosensor.

So we can write,

$$|Z| = Z_1 \quad (4)$$

At higher frequencies 500 KHz- 1 GHz,  $C_{de}$  dominates the total impedance. As the frequency increases, the effect of  $C_{dl}$  is minimized. Thus the impedance almost equals the resistance of the test solution.

$$|Z| = R_{sol} \quad (5)$$

## 2.2 Dielectrophoresis for Cell Separation

In many biomedical applications Dielectrophoresis (DEP) has certain advantages over traditional techniques of cell separation. Using DEP, we can isolate and analyze a wide range of particle types (cells, bacteria, viruses, DNA and proteins) without harming them. DEP has the ability to operate directly on unaltered, unlabeled cells. Thus it reduces the expense, labor and time required for the development and validation of labeling and tagging. DEP doesn't affect the properties of the cells. As a result the cells remain viable for further analysis [44].

Polarized charges are induced on the surface of a dielectric particle when it is subjected to an electric field. This polarized charges cause an electric dipole to be generated. The magnitude and the direction of these induced dipoles depend on many factors such as the magnitude and the frequency of the electric field in which the dielectric particle is suspended. When the electric field is uniform, equal Coulomb forces

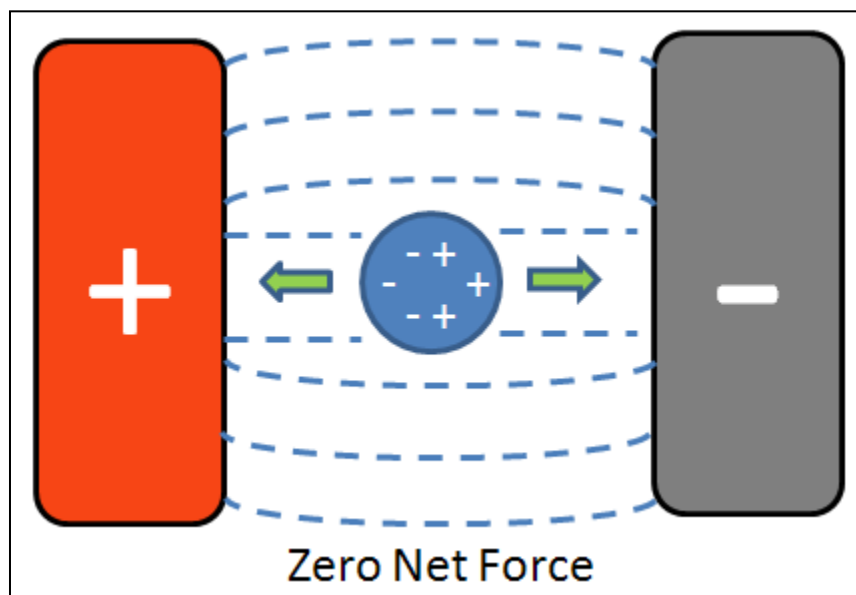
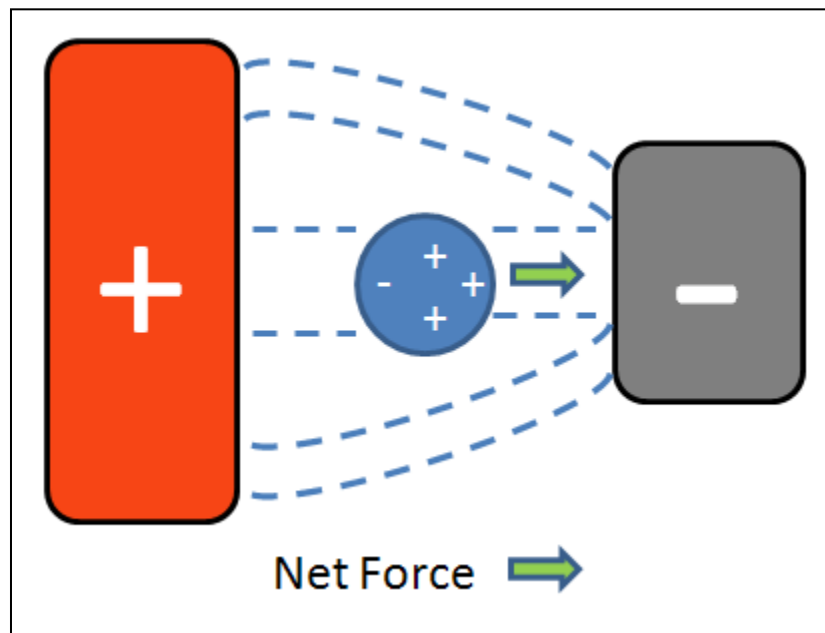


Figure 2.3 Dipole movement (Equal and Opposite dipoles).

are generated on both side of the dielectric particle. As the forces are equal in magnitude but opposite in direction they nullify each other [45]. But if the electric field is non-uniform, the Coulomb forces generated on the opposite sides are not equal to each other. This generates a resultant force which provides motion to the particle. The direction of the resultant force depends on the electric field. So, dielectrophoresis (DEP) can be defined as the polarization associated to the motion induced in particles by a non-uniform electric field. If the polarizability of the particle is more than that of the surrounding medium, it is called positive dielectrophoresis (pDEP) and the particle tends to move towards the region of high field strength.



**Figure 2.4 Dipole movement (Unequal and Opposite Dipoles)**

On the other hand if the particle is less polarizable than the surrounding medium the phenomenon is termed negative dielectrophoresis (nDEP) and the particle tends to move towards the region of low field strength. Figure 2.4 shows the phenomenon of positive and negative dielectrophoresis on particles under the influence of applied electric field. If

the polarizability of the particle is more than that of the surrounding medium, it is called positive dielectrophoresis (pDEP) and the particle tends to move towards the region of high field strength. On the other hand if the particle is less polarizable than the surrounding medium the phenomenon is termed negative dielectrophoresis (nDEP) and the particle tends to move towards the region of low field strength. Figure 2.4 shows the phenomenon of positive and negative dielectrophoresis on particles under the influence of applied electric field.

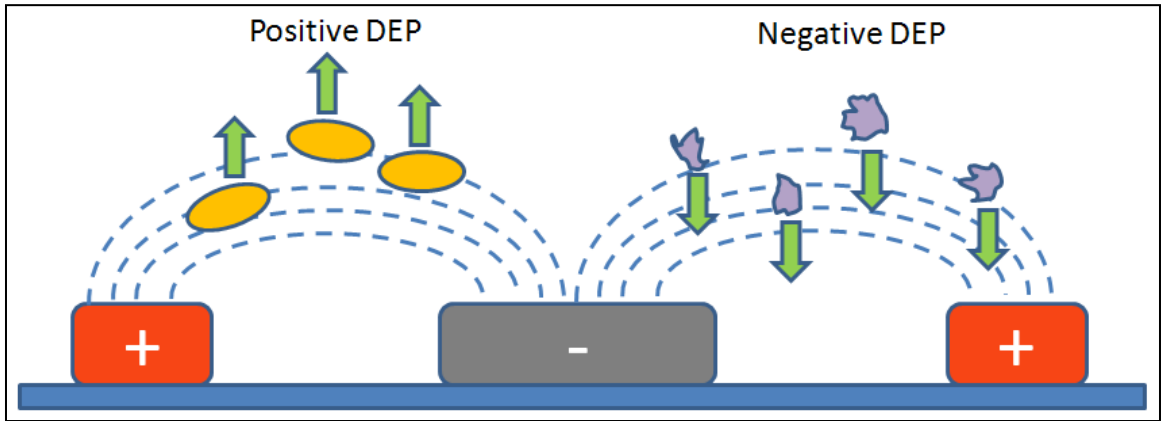


**Figure 2.5 Schematic diagram showing the positive and negative dielectrophoretic forces on particles subjected to non-uniform electric fields.**

The dielectric force ( $F_{DEP}$ ) on a homogeneous spherical particle can be expressed by the following equation,

$$F_{DEP} = 2\Pi R^3 \epsilon_m K(\omega) \nabla |\overline{E_{RMS}}|^2 \quad (6)$$

Where  $R$  = radius of the sphere,  $\epsilon_m$  = complex permittivity of medium,  $|\overline{E_{RMS}}|$  = RMS value of the electric field.  $K(\omega)$  is called the Clausius-Mossotti (C-M) function and can be defined using the following equation.

$$K(\omega) = \frac{\epsilon_p^* - \epsilon_m^*}{\epsilon_p^* + 2\epsilon_m^*} \quad (7)$$

$$\boldsymbol{\varepsilon}^* = \boldsymbol{\varepsilon} - \frac{i\sigma}{\omega} \quad (8)$$

Therefore the C-M function can be written as,

$$K(\omega) = \frac{(\varepsilon_p - \frac{i\sigma_p}{\omega}) - (\varepsilon_m - \frac{i\sigma_m}{\omega})}{(\varepsilon_p - \frac{i\sigma}{\omega}) + 2(\varepsilon_m - \frac{i\sigma}{\omega})} \quad (9)$$

$$K(\omega) = \frac{(\varepsilon_p - \varepsilon_m) - i(\frac{\sigma_p - \sigma_m}{\omega})}{(\varepsilon_p + 2\varepsilon_m) - i(\frac{\sigma_p + 2\sigma_m}{\omega})} \quad (10)$$

where,  $\varepsilon$  = permittivity,

$\sigma$  = conductivity,

$\omega$  = angular frequency

$i$  = imaginary number or  $\sqrt{-1}$ .

Replacing the derived value of C-M function on equation X the dielectrophoretic force can be rewritten as,

$$F_{DEP} = 2\Pi R^3 \varepsilon_m \left\{ \frac{(\varepsilon_p - \varepsilon_m) - i(\frac{\sigma_p - \sigma_m}{\omega})}{(\varepsilon_p + 2\varepsilon_m) - i(\frac{\sigma_p + 2\sigma_m}{\omega})} \right\} \nabla |\overline{\mathbf{E}_{RMS}}|^2 \quad (11)$$

The dielectrophoretic force depends on the real part of the C-M function. The imaginary part of the function determines the electrorotational force.

### **2.3 Bacteria Detection Mechanism: Impedance Spectroscopy**

A high density interdigitated electrode array is used to detect different concentrations of *E. coli* O157:H7 in solution. The surfaces of the electrodes are functionalized and modified using specific antibodies. The antibody binds to the surface of the electrodes through non-specific absorption. This surface modified electrodes form a biological transducer. When the test solution comes in contact with the electrodes, the target cells (antigen) present in the test sample binds to the antibodies immobilized to the electrode surface. The presence of bacteria on the surface causes the impedance measured across the electrodes to change. The impedance change can be measured and correlated to the target cells concentration. The impedance measurement is performed using an impedance analyzer. The measured impedance response is displayed in graphical format for various frequency points. At higher frequencies the impedance response is solely due to the dielectric capacitance and the effect of bacteria cells is insignificant. But in lower frequency ranges the impedance response is significantly affected by the amount of bacteria present in the test solution. Thus impedance measurement and analysis is performed in the range of 100Hz to 1GHz to understand the effect of the biosensor in both low and high frequency bands.

## CHAPTER 3: Design and Modeling

This chapter will introduce and describe the two different biosensor designs for detection of *E.coli O157:H7*. The layout for both the designs has been drawn using L-EDIT CAD tool. Simulations were performed using Finite Element Machine (FEM) model using Coventorware<sup>TM</sup> software prior to device fabrication. The relationship between the width-spacing of electrode fingers and the field strength of the effective electromagnetic force has been studied using simulations.

### 3.1 Biosensor Design

Two different designs for the biosensor are presented in this thesis. Both variations of the biosensor use interdigitated electrode array to detect the presence of *E.coli O157:H7* cells in a test solution as interdigitated electrodes have certain advantages compared to other electrode systems. Unlike most microelectrode based biosensors, in these designs, microchannels are used to flow the test solution through the microelectrode array. Microchannel increases the efficiency and reliability of the biosensor as it isolates the test solution from surrounding environment thus reducing the possibility of interference and noise during impedance measurement. Also by using microchannel to flow the test sample, the test volume can be controlled precisely. Although both of these

biosensors use similar principals for impedance based detection of *E.coli* 0157:H7, there are some major differences between the two. The first design is based on a planar 2-dimensional (2-D) IDAM whereas the second design has two sets of 3-dimensional (3-D) IDAM arrays. The Interdigitated electrode array in Design-I is planar (2-D), whereas electrode array in Design-II has 3-dimensional structure. The structure of the microchannel is also different in both designs. In the first design the microchannel flows to top of the electrodes, but in the second 3-D design the IDAM surrounds the microchannel in all four directions. In Design-1 the microchannel is embedded in Polydimethylsiloxane (PDMS), but in Design-II the channel is made of AZ 4620, SU-8 and the PDMS layer surrounded by 3-D electrode array. PDMS is chosen because of its excellent biocompatibility and ease of fabrication. It is transparent in visible and UV light spectrum and since it is a polymer it is highly flexible and conforms to the curvature of the surface it comes into contact with. Interdigitated electrodes array is made of Gold as it is a noble metal and has very good electrical properties and also posseses excellent biocompatibility.

### **3.1.1 Biosensor Design-I**

The first design of the biosensor consists of a planar interdigitated electrode array and a microchannel. A thin film of gold layer on a glass substrate is used to construct the high density interdigitated electrode array. A straight microchannel is used to flow the test sample on the electrode array. Inlet and outlet are present on two opposite ends of the microchannel. The test sample is injected in the microchannel through the inlet and it is directed towards the planar interdigitated electrode array. The electrode surface is modified by immobilizing *anti-E.coli* antibody on them. As different test samples



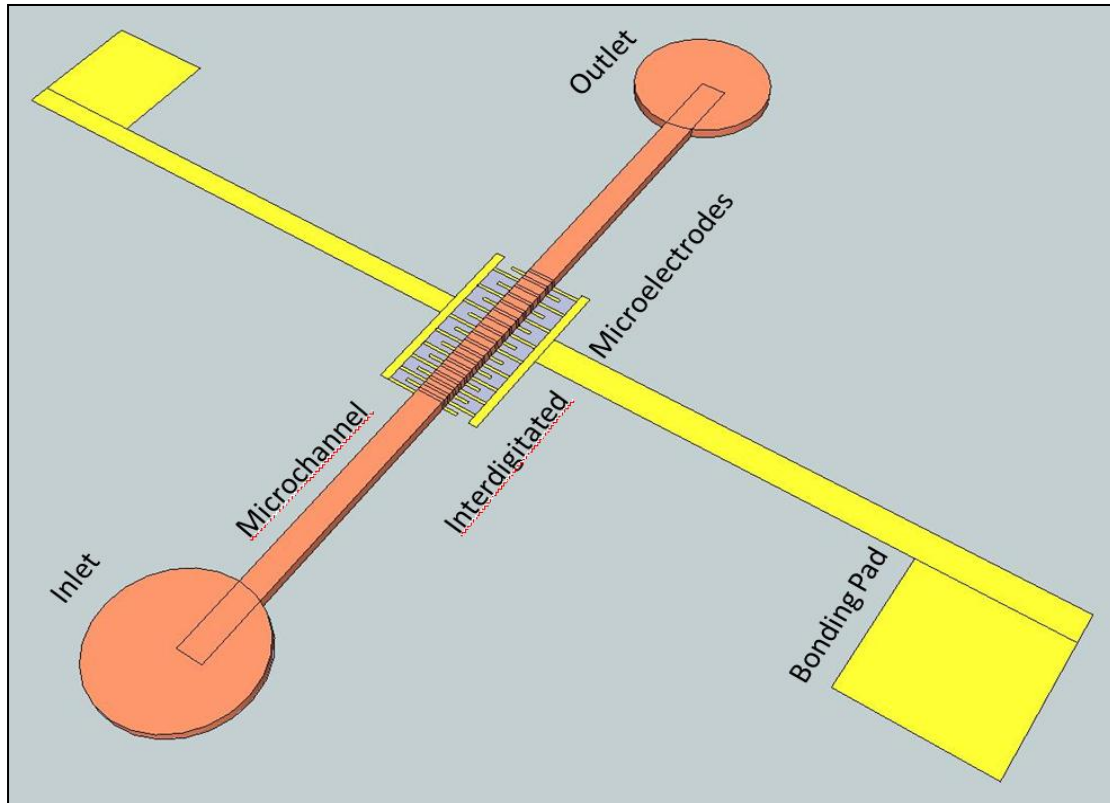


**Figure 3.1 Biosensor Design – I**

contaminated with *E.coli* O157:H7 are flown through the device, the cells tend to bind to the surface of the electrodes. The presence of the cells on the electrodes causes a change in the impedance. Because the interdigitated electrode array is used to detect the presence of *E.coli* O157:H7 bacteria, it is called the detection array.

### **3.1.2 Biosensor Design-II**

The second design is quite different compared to the first one. Unlike the planar (2-D) interdigitated electrode array of Design-I the electrode array in this design has a 3-dimensional (3-D) interdigitated detection array. To improve the efficiency of detection in this design, dielectrophoresis is used to separate the *E.coli* O157:H7 cells from unwanted objects present in the test solution. To perform dielectrophoresis, an additional

array of 3-dimensional interdigitated electrodes is also present in this design. This array of interdigitated electrodes is called the focusing array. The structure of the microchannel

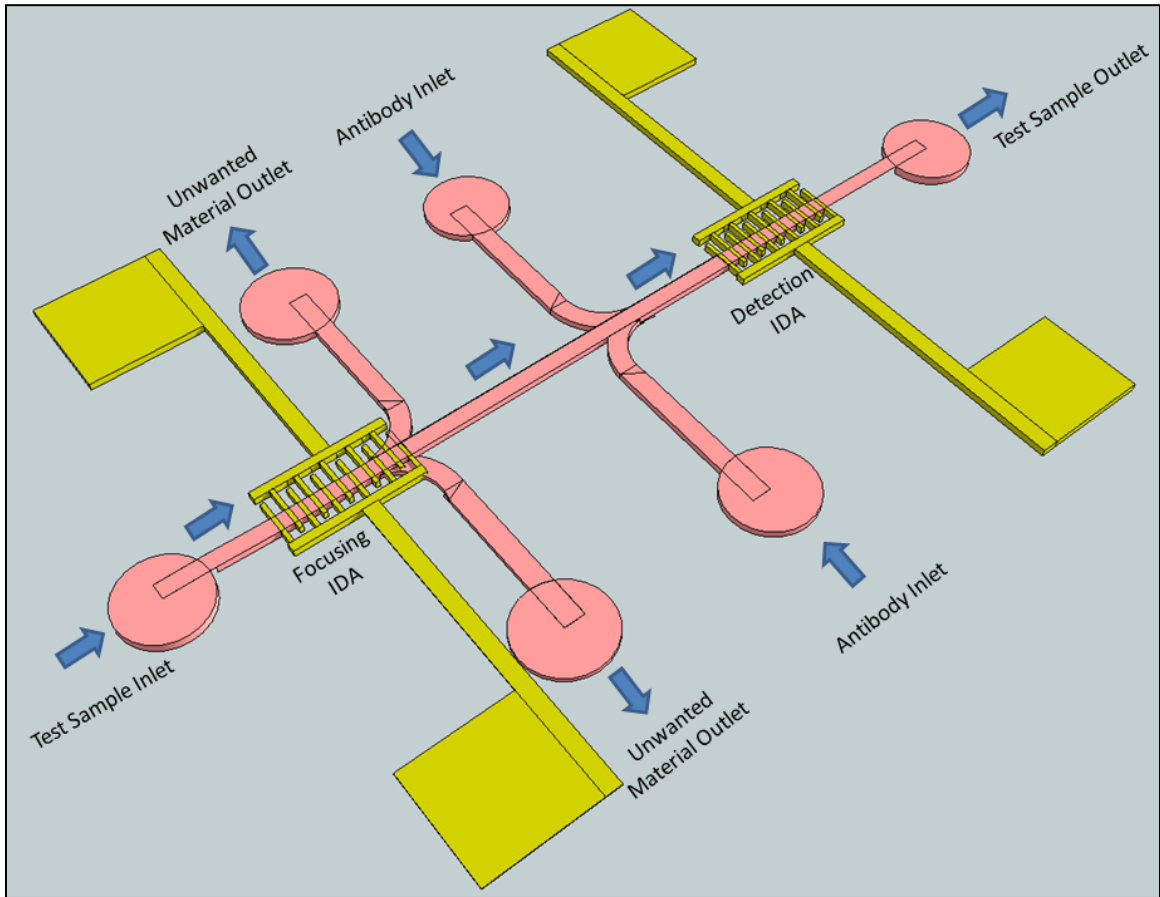


**Figure 3.2 Biosensor Design – II**

is also different than the first design. The microchannel has an inlet and outlet and also two additional pairs of fluidics port. The first pair of fluidics port is used as an outlet for unwanted objects separated from the test solution after dielectrophoresis. The second pair of fluidics port is used to inject antibody solution into the microchannel to coat the electrodes surface in the detection array with *anti-E.coli* antibody. To perform impedance measurement and to detect *E.coli O157:H7*, the test solution is pumped into the microchannel through the inlet. The solution when passing through the detection array, experiences a dielectrophoretic force which concentrates the *E.coli O157:H7* cells

towards the center of the channel. These cells continue to flow with the solution through the center of the channel towards the detection array. The unwanted objects come out through the unwanted object outlets. As the electrode surfaces are coated with *anti-E.coli antibody* the *E.coli O157:H7* cells tend to bind on the electrodes resulting in an impedance change. The obtained impedance response in this case is much more refined as it is mostly due to the *E.coli O157:H7* cells. After the impedance measurement is performed the test solution comes out through the outlet. This design of the biosensor with 3-D electrode array increases the sensing surface to volume ratio compared to the 2-dimensional (2-D) biosensor. This increased surface to volume ratio enhances the sensitivity of impedance detection, and is also capable to confine a few live bacterial cells in a small volume.

### **3.2 Layout Designing Using CAD Tools**

Fabrication of a MEMS device involves several stages of development. Among these, layout designing is a very important step towards the fabrication of the device. Multiple steps are incorporated together to fabricate a MEMS device and several masks are required for different stages of fabrication.

L-Edit CAD tool was used to design the layouts for the interdigitated microelectrode array and the fluidic microchannel. The layouts were then printed on a transparency using 1/65 mil Precision Laser Photoplot. Using these transparencies hard masks (quartz) were fabricated as hard masks provides better precision during fabrication of smaller and high density features.

For Design-I of the biosensor, two masks are created. ‘Mask 1’ is for the fabrication of high density interdigitated electrode array. In this design the interdigitated

electrode array has 100 pairs of electrodes (Figure 3.3(a)). Each of these electrodes has length and width of  $1500\mu\text{m}$  and  $10\mu\text{m}$  respectively. The spacing in-between the electrodes is  $10\mu\text{m}$ .

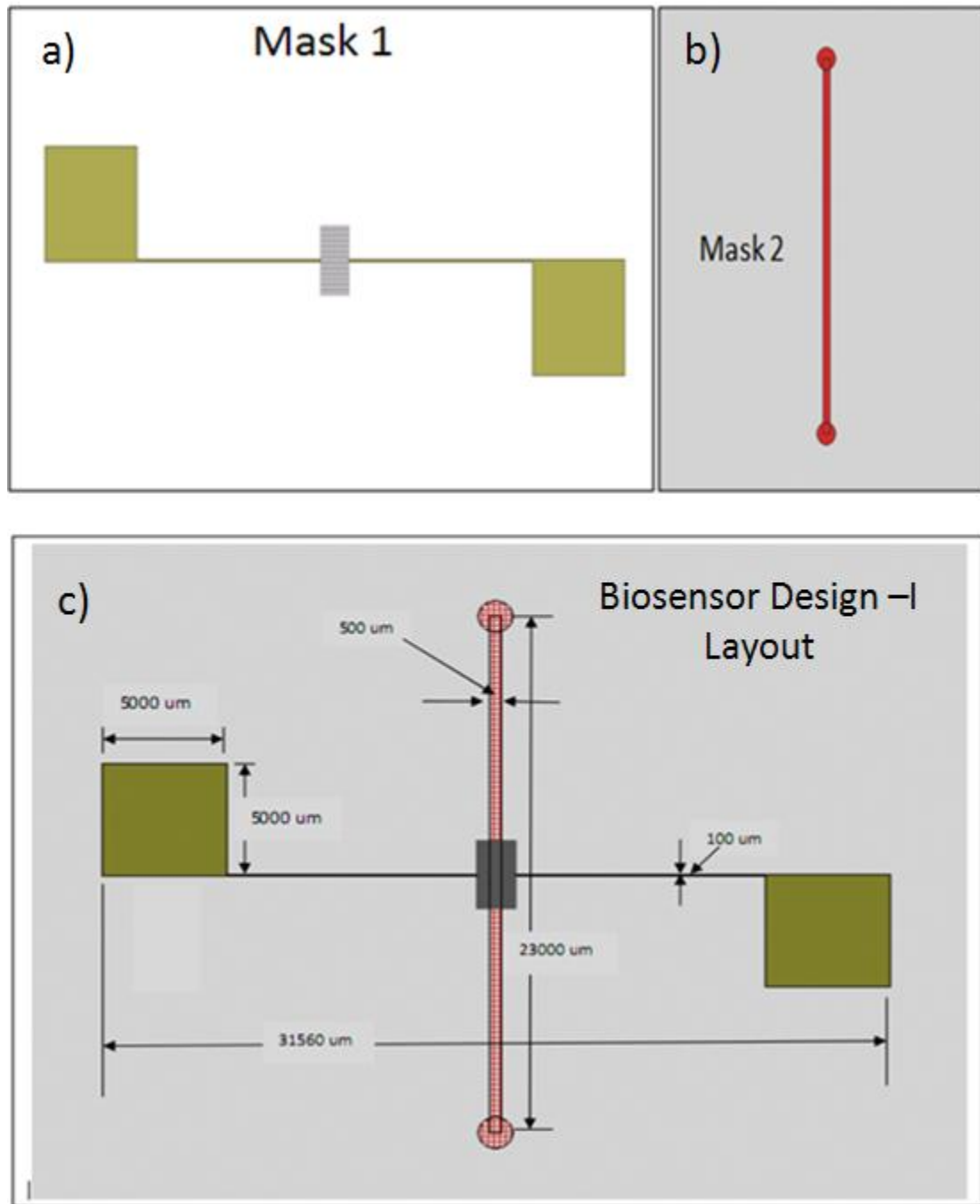


**Figure 3.3 Biosensor Design – I Layouts a) Magnified view of Interdigitated Microelectrode b) Microchannel c) Design – I entire layout**

The second mask, 'Mask-2' is for the fabrication of the fluidic microchannel. It is a straight channel with inlet and outlet on the two opposite ends. The microchannel used in this design has a width and depth of 500  $\mu\text{m}$  and 50  $\mu\text{m}$  respectively (Figure 3.3(b)). Both the masks are superimposed and the entire of the device is shown in Figure 3.3(c)

The second design of the biosensor (Design-II) also requires two masks, which are shown in Figure 3.4(a) and Figure 3.4(b). 'Mask 1' is used to fabricate the high density electrode arrays. Unlike the electrode Mask of Design-I, this mask consists of two sets of electrodes. The first array has 100 pairs of electrodes and the second one has 25 pairs. Each electrode is 500  $\mu\text{m}$  long and has a width of 10  $\mu\text{m}$ . The inter-electrode spacing is 10  $\mu\text{m}$ . Each set of electrode array has a pair of bonding pads for electrical connections. The larger array of electrode has been designed for dielectrophoretic focusing of the cells and the smaller array for detection purpose.

'Mask 2' is the mask for fabricating the fluidic microchannel of Design-II. The microchannel in Design-II is more complex compared to the previous design. It consists of 2 set of branches and six inlet-outlet ports. The first set of branches is used as outlets for objects which are filtered out from the cell solution using dielectrophoresis. The second set of branches is used to send antibody solution and immobilize antibodies on the detection array. The microchannel has variable width throughout its length. Towards the beginning, the width of the microchannel is 300  $\mu\text{m}$ . The branches and the remaining part of the channel have width of 100  $\mu\text{m}$ . The depth of the channel is 25  $\mu\text{m}$ . Figure 3.5(a) and Figure 3.5(b) shows the entire layout of the device.

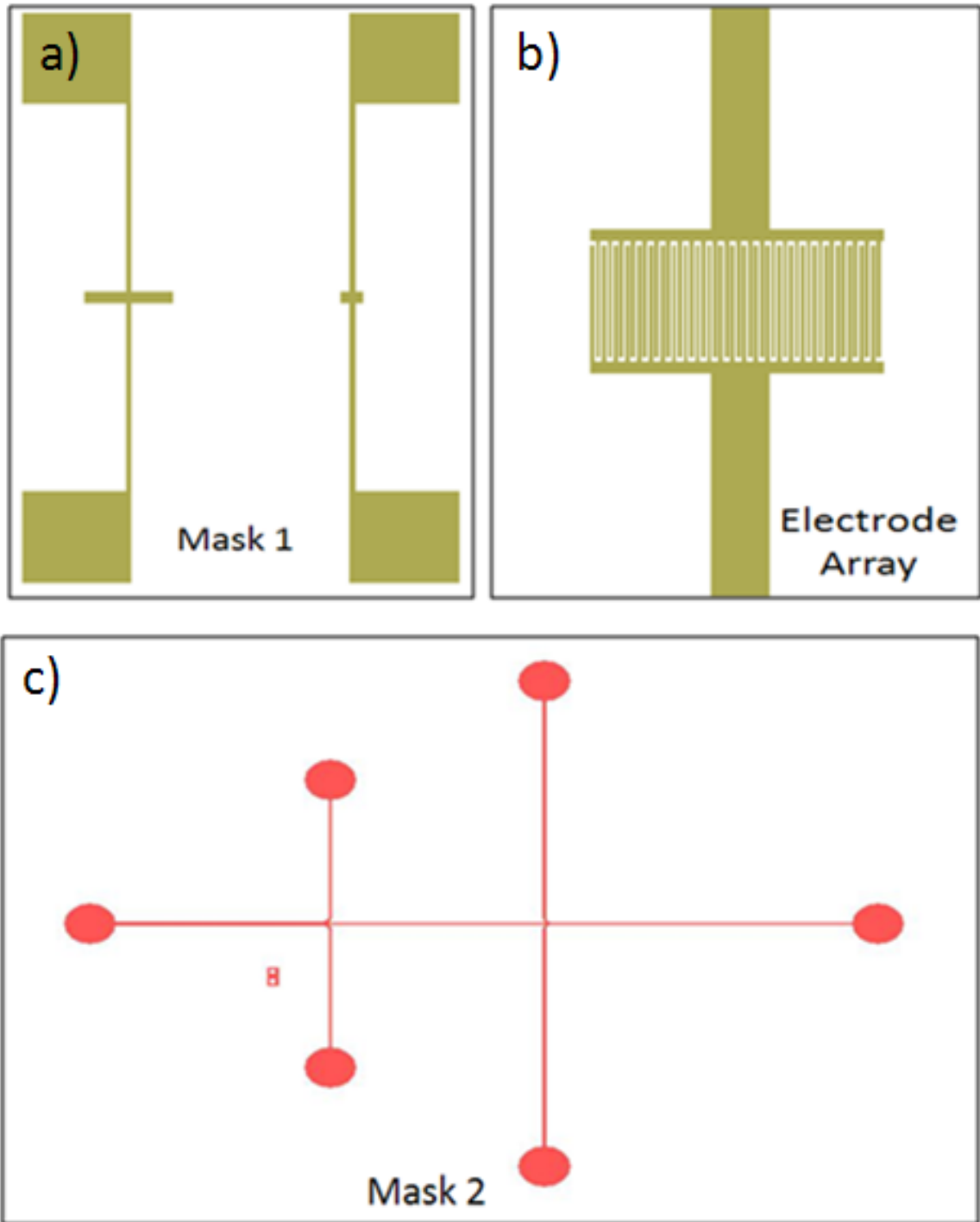


Figure 3.4 Biosensor Design – II Layouts a) Interdigitated Microelectrodes b) Magnified view of Interdigitated Microelectrode c) Microchannel

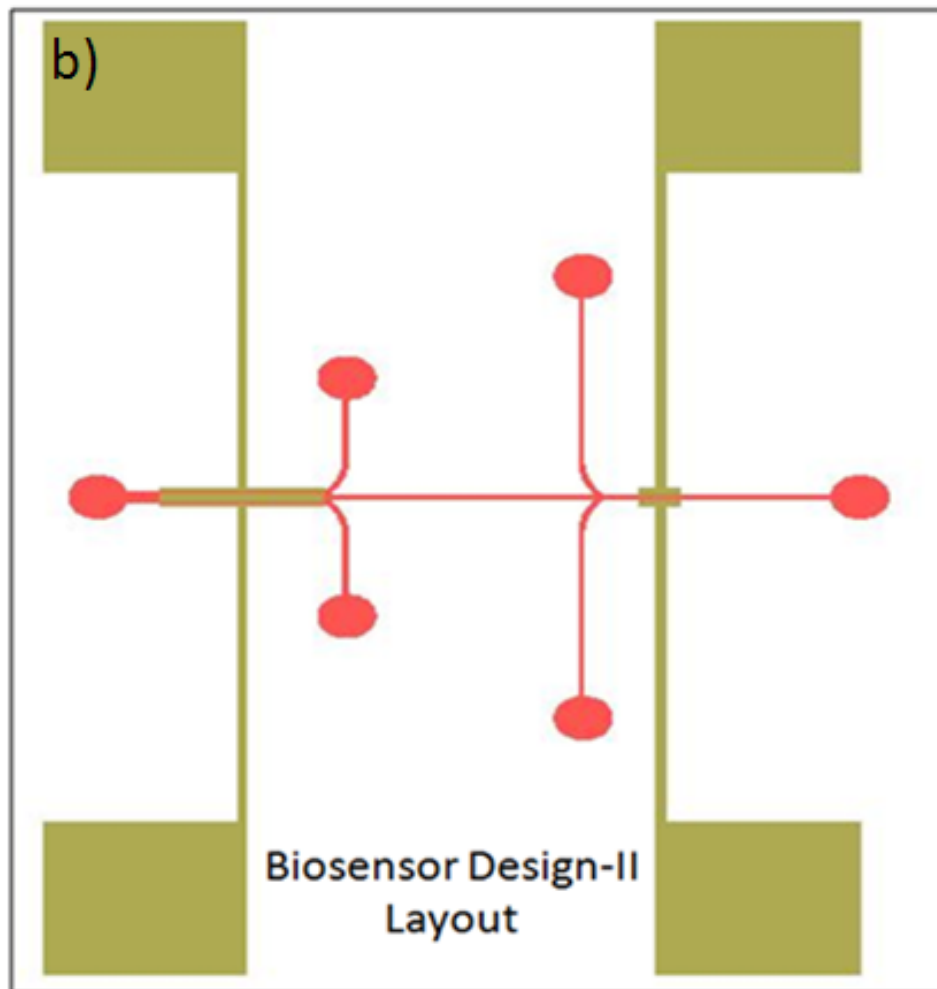
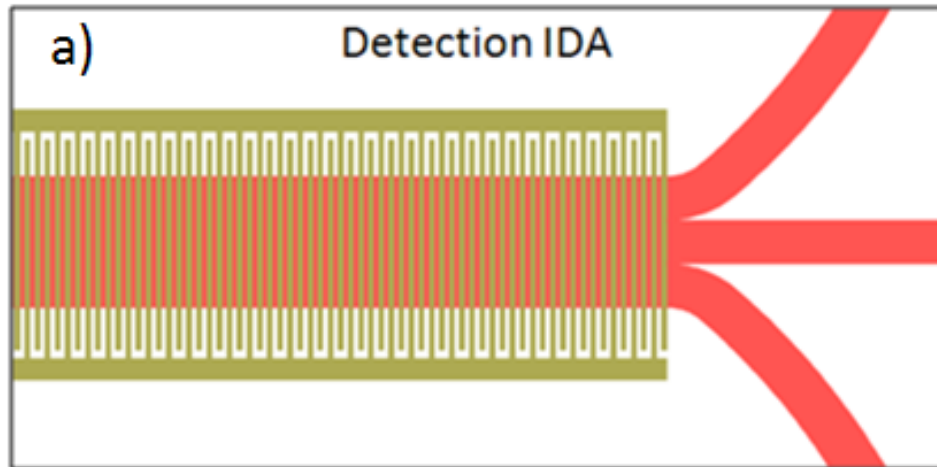


Figure 3.5 a) Focusing IDA with Microchannel b) Complete layout of Design – II

### 3.3 Electric Field Modeling

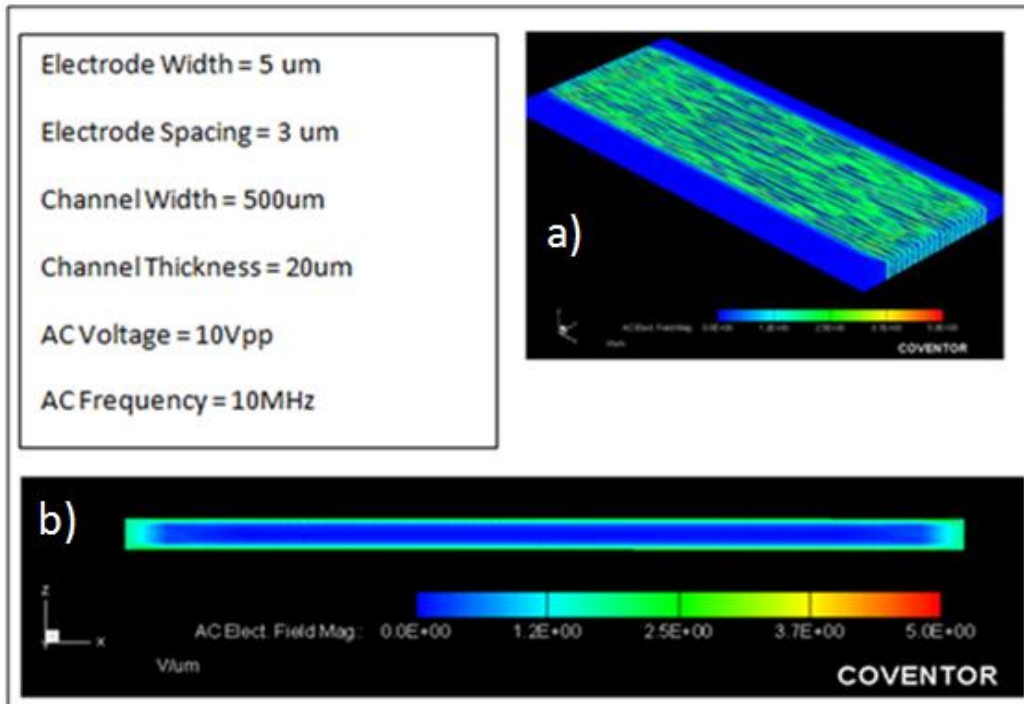


Figure 3.6 Electric field distribution across focusing electrode array a) Three dimensional view, b) Cross section view.

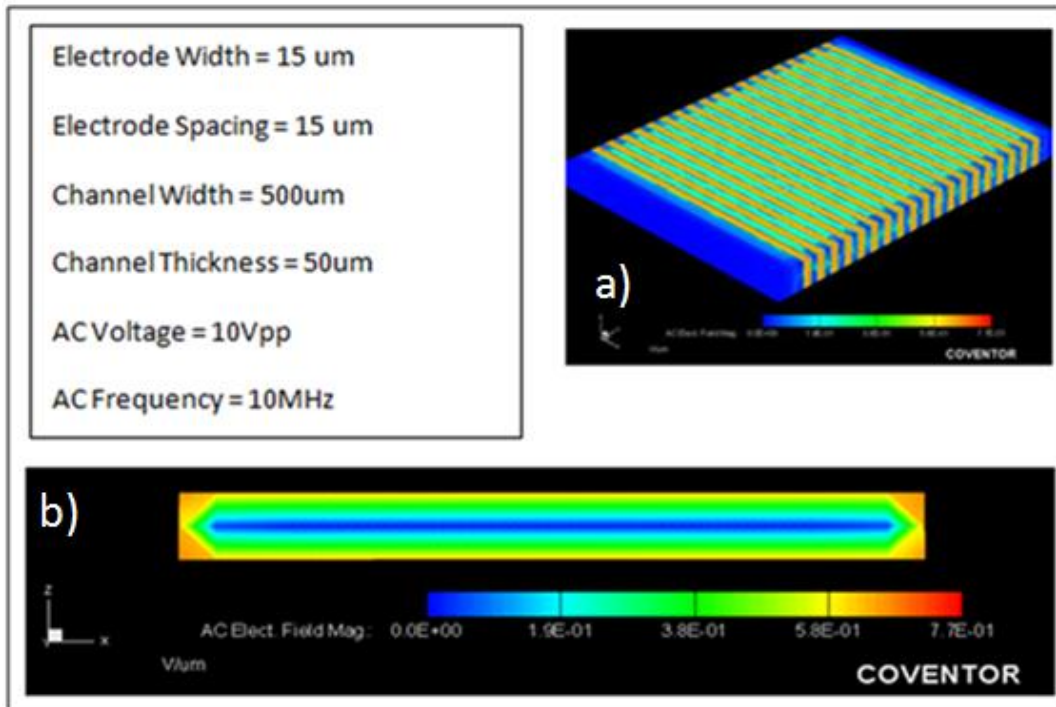


Figure 3.7 Electric field distribution across focusing electrode array a) Three dimensional view, b) Cross section view.



Using dielectrophoresis unwanted objects can be separated from the cell solution when subject to non-uniform electric field distribution. This feature of cell separation is utilized in 'Design-II' of the biosensor. Dielectrophoresis is dependent on the behavior of the electric field. Thus it is important to run simulations and study the behavior of the electric field generated by the interdigitated electrode array. CoventorWare 2008, a MEMS design, simulation and analysis software was used for this purpose. In Coventorware NetFlow (Electrokinetic) and MemCFD (Fluid Dynamics) modules were used to perform Finite Element Model (FEM) analysis. Fluent solver was used to study the distribution of the electric field generated by the focusing electrode array (Figure 3.6 and Figure 3.7). From the simulation it was found that the electric field is non-uniform. It was also observed that the field strength is higher at the edges of the electrodes and gradually decreases moving towards the center of the channel. Due to this non-uniform distribution of electric field strength dielectrophoresis forces are generated. This force acts on the unwanted objects and move them towards the higher electric field region. These unwanted objects then be directed toward the 'Unwanted Material Outlet'. The bulk fluid which will contain majority of the bacteria will keep flowing toward the detection array of electrodes.

## **CHAPTER 4: Fabrication of Biosensor**

Micromachining and micro-electromechanical system (MEMS) technologies can be used to produce complex structures, devices and systems on the scale of micrometers. Initially micromachining techniques were borrowed directly from the integrated circuit (IC) industry, but now many unique MEMS specific micromachining processes are being developed. [1]

### **4.1 Materials Used in the Fabrication**

Biosensors are often subject to experiments involving biochemical and biological processes. Materials used in construction of the biosensor play a very important role. If the proper materials are not chosen it may yield unwanted results. Thus the success of the biosensor depends on the choice of right biocompatible materials.

#### **4.1.1 Glass Slide**

The biosensor is constructed on a regular microscopic glass slide. The glass slide is used as a base-substrate for the device. There are many reasons for choosing glass as substrate.

Glass has an excellent biocompatibility and also serves as a transparent medium for photosensitive experiments.

#### **4.1.2 Metals**

Metals are very important components of many biosensors and biomedical devices. In our device the interdigitated electrodes are made of metals. The metal electrodes remain in direct contact with the biological samples. So the biocompatibility of these metal electrodes is a high priority. The two metals which are used to construct the electrodes are Chromium (Cr) and Gold (Au). Gold has an excellent biocompatibility, but Chromium is known to be non-biocompatible. Although Chromium is not a very good biocompatible metal, the construction of the biosensor still allows us to use Chromium as it gets completely covered by the gold layer and doesn't come in direct contact with the biological compounds.

##### **4.1.2.1 Chromium**

The gold-to-glass adhesion remains a key problem, due to the difficulty of forming a direct bond between the film and substrate. Thus, gold and other noble metal coatings on glass are usually applied with the interposition of double Cr/Ni layers after various etching/cleaning steps [46]. So to promote the adhesion between the Gold and Glass a thin layer of Chromium is introduced. The Chromium is deposited up to a thickness of 40 nm using Kurtluskor co-deposition sputtering system.

#### **4.1.2.2 Gold**

Gold is a noble metal. It has the highest malleability and ductility among all metals. Also it is resistant to oxidation in air or water. Moreover it is a very good conductor and an excellent biocompatible metal. All these features make it an excellent choice for the interdigitated electrode. The Kurtluser co-deposition sputtering system is used to deposit a uniform layer (~140 nm) of Gold on top of the Chromium Layer.

#### **4.1.3 Polydimethylsiloxane (PDMS)**

The handling and delivery of small quantities of liquid is a critical part of many physical, chemical, and biological processes, both in the laboratory and in Nature [47]. From a microfluidics point of view, shallow microchannels inevitably result in large pressure drops and large shear stresses (Potter and Foss, 1982) requiring strong sealing, high injection pressures, and/or low flow rates. [46]. Creating micro channels by etching glass and Si is expensive and a slow process. Moreover Si is opaque and unsuitable for photosensitive experiments.

Researchers have continuously looked for new materials and methods for effective fabrication and utilization of micro channels. In the last few years, Polydimethylsiloxane (PDMS) has been largely employed for implementation of microfluidic devices. The advantages of PDMS are many: optical transparency in a broad range of spectrum, bio and chemical compatibility with safe use, low cost, easy and superior bonding property, low water permeability and simple processing using the micro molding technique [48]. In our device, the microchannel is embedded in the PDMS layer. The depth of the channel is ~50  $\mu\text{m}$ .

## 4.2 Fabrication

The fabrication process of the biosensor is a conjunction of various methods used in the semiconductor integrated circuit industry. The fabrication process has been graphically illustrated in Figure. 4.1.

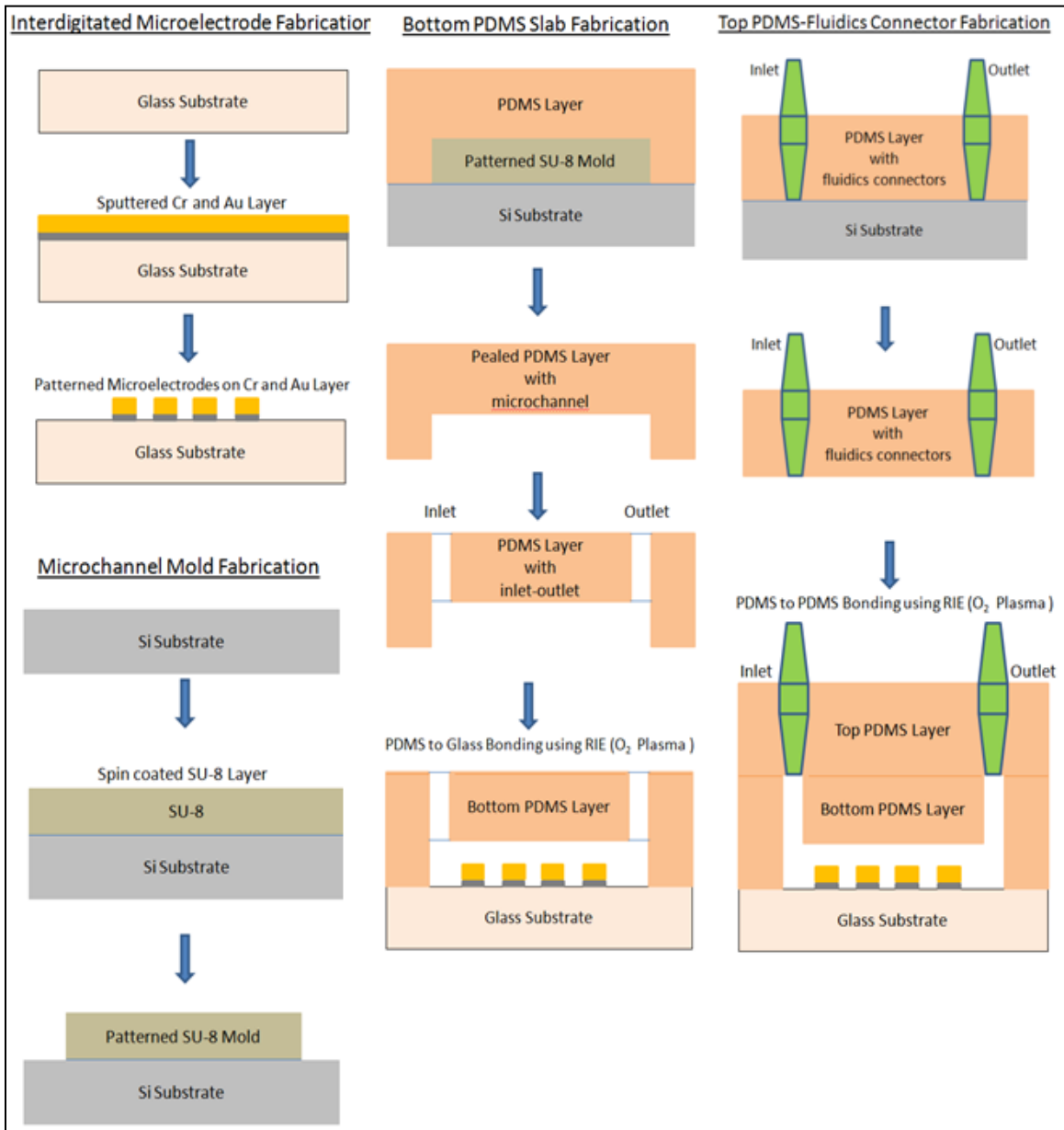
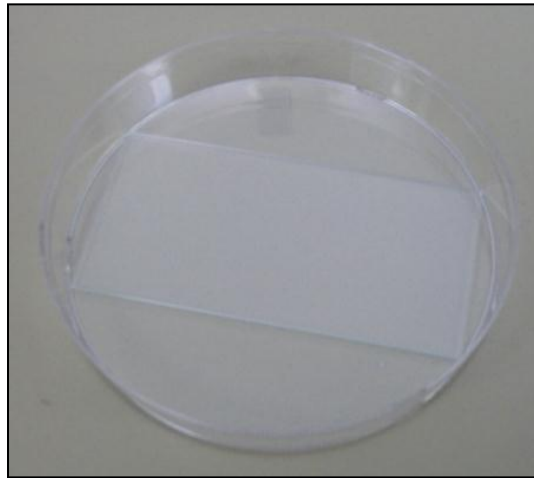


Figure 4.1 Crosssectional view of Fabrication Process

#### **4.2.1 Surface Purification of Glass Slide**

A regular microscopic glass slide is used as the base substrate for the biosensor(Figure 4.2). The first step in fabricating is to purify the surface of the glass slide on which the biosensor will be constructed. To perform this step, a unique solution called Piranha etch is used which is a mixture (3:1) of sulfuric acid ( $H_2SO_4$ ) and hydrogen peroxide ( $H_2O_2$ ). The solution is a strong oxidizer and removes almost any organic substance present on the glass substrate.



**Figure 4.2 Piranha cleaned Glass slide**

The surface of the glass slide on which the biosensor will be constructed is faced up and emerged into the solution for a period of 3 minutes. This is followed immediately by washing with distilled water (DI) to remove any piranha etch residue.

#### **4.2.2 Deposition of Metals**

Once the surface purification is performed the metals Chromium and Gold are deposited on the glass slide. The process of deposition used is Sputtering. Sputtering is a Physical vapor Deposition process to deposit a uniform thin film on a substrate. There are several types of sputtering processes, including ion beam, diode and magnetron sputtering.

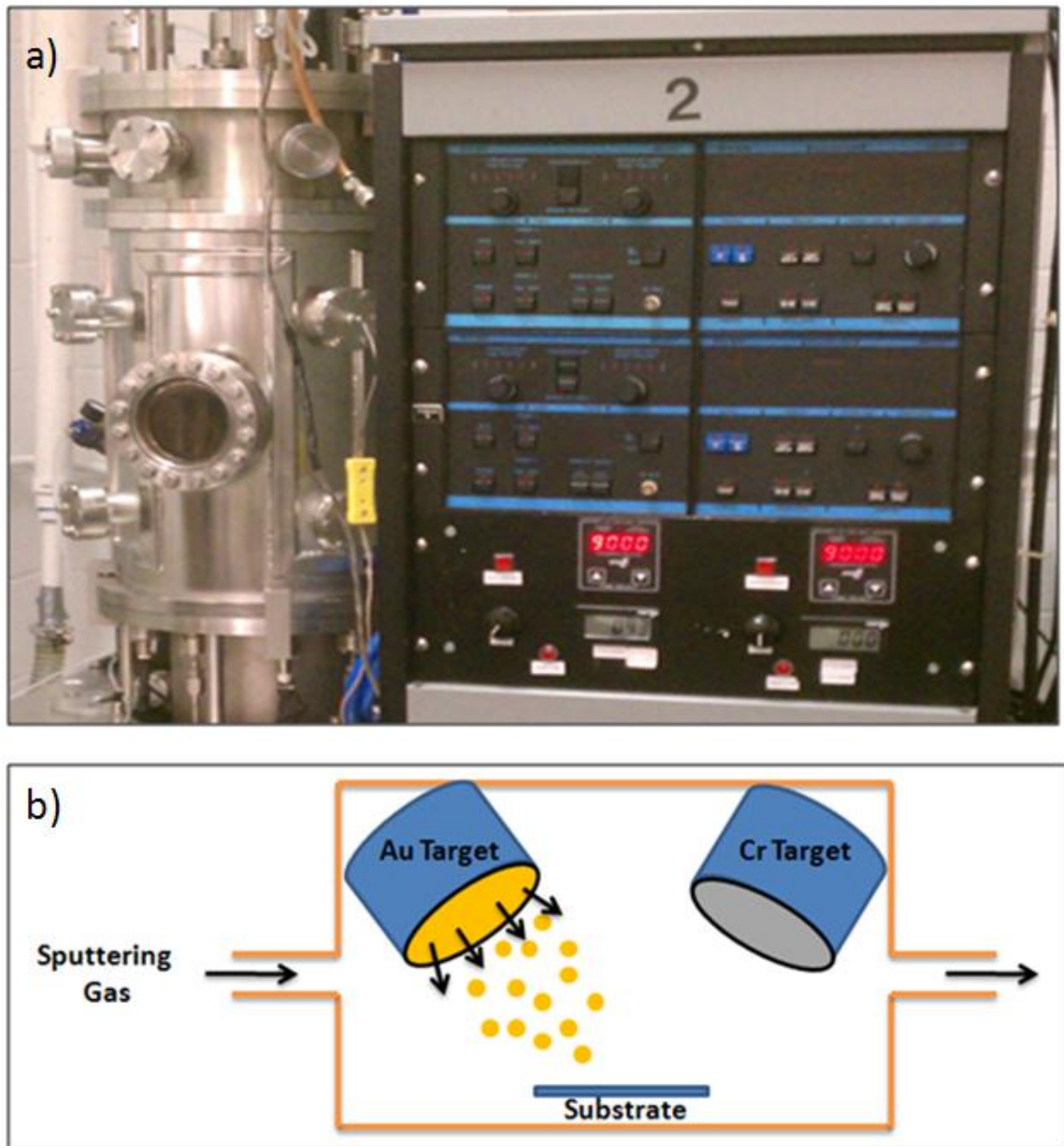


**Figure 4.3 a) Sputtering system b) Graphical illustration of Sputtering**

The sputtering system used for fabricate this biosensor is shown in Fig. 4.2. In this sputtering system, high voltage is delivered across a low pressure gas, Argon (Ar), to generate the high energy plasma. The plasma emits a colorful halo of light often referred to as a "glow discharge". These energized plasma ions strike the target materials

(Chromium and Gold), ejects them from the target and bonds on the surface of the glass substrate.

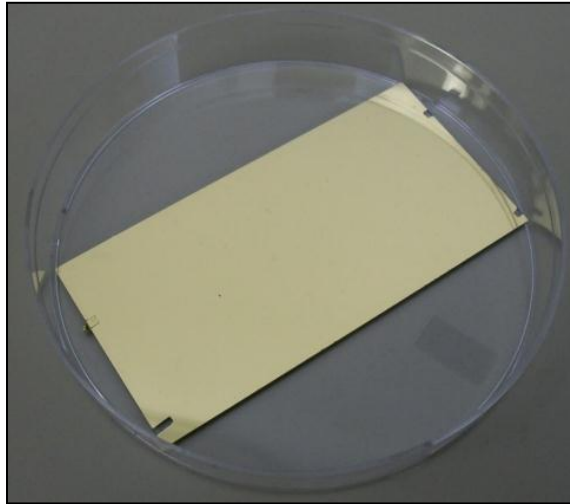


**Figure 4.4 Glass slide sputtered with Cr and Au**

The sputtered glass slide is shown in Fig 4.4. A uniform thin film of Cr (40 nm) is deposited on the surface of the glass slide, followed by a thin layer of Au (140 nm). The Au layer completely covers the Cr layer and prevents it from coming in contact with the biological samples.

### **4.2.3 Photolithography**

Photolithography is a very important process in MEMS fabrication industry. It is used to pattern photosensitive organic material called photoresist to obtain desired design or pattern on the substrate. A chromium hard mask is used to create the pattern. Photoresist can be of two different types, positive and negative. Depending on which photoresist is used we may obtain either a positive or negative image of the mask on the substrate. To pattern the interdigitated electrodes on the deposited metals we need to



perform the photolithography process. The metal deposited glass slide is first spin coated with a positive photoresist layer, Shipley 1813. This is performed using Brewer Science 200X Precision Spincoater for 25 seconds at 3000 rpm. The samples are then

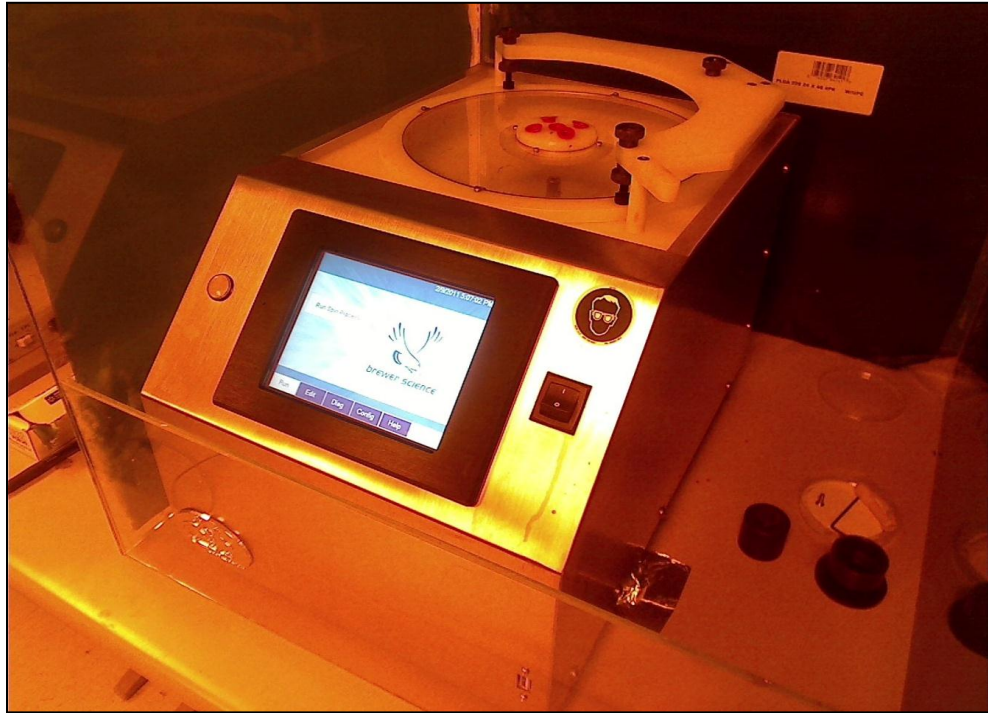


**Figure 4.5 Spincoater used for photoresist coating**

immediately soft baked for 1 minute at 90°C. Wait time of one minute allows the samples to rehydrate before exposure. Karl Suss MJB3 Maskaligner is used to expose the samples to UV light. After exposure is complete the samples are immediately developed for 35 seconds using developer MF-319 and thoroughly rinsed with DI water. After this step we have the photoresist patterned in shape of interdigitated electrodes

#### **4.2.4 Patterning Interdigitated Electrode Arrays, Traces and Bonding Pads**

The Interdigitated electrodes are patterned with the help of a process called Etching. Etching removes unwanted material either physically or chemically from the

surface of a substrate. It is a widely practiced process in MEMS industry. Etching can be classified into two major types, wet etching and dry etching. The etching process which



**Figure 4.6 Maskaligner used for photolithography**

we use in fabrication of the biosensor is a wet etching process. The etching is performed in two steps. First the Au layer is etched followed by the Cr layer. The glass slide with the patterned photoresist is emerged in the Gold Etchant solution until the unwanted gold is removed from the surface and is immediately rinsed with DI water. Cr is etched with Chromium Etchant in similar fashion. After etching the sample is thoroughly rinsed with DI water. The sample is than thoroughly rinsed with Acetone and IPA to remove the photoresist layer which leaves the developed and patterned interdigitated electrodes on the glass slide. After the photoresist is removed from the gold surface the sample is dried using  $N_2$ . Different views of the patterned electrodes are shown in Figure. 4.7, Figure. 4.8 and Fig. 4.9.

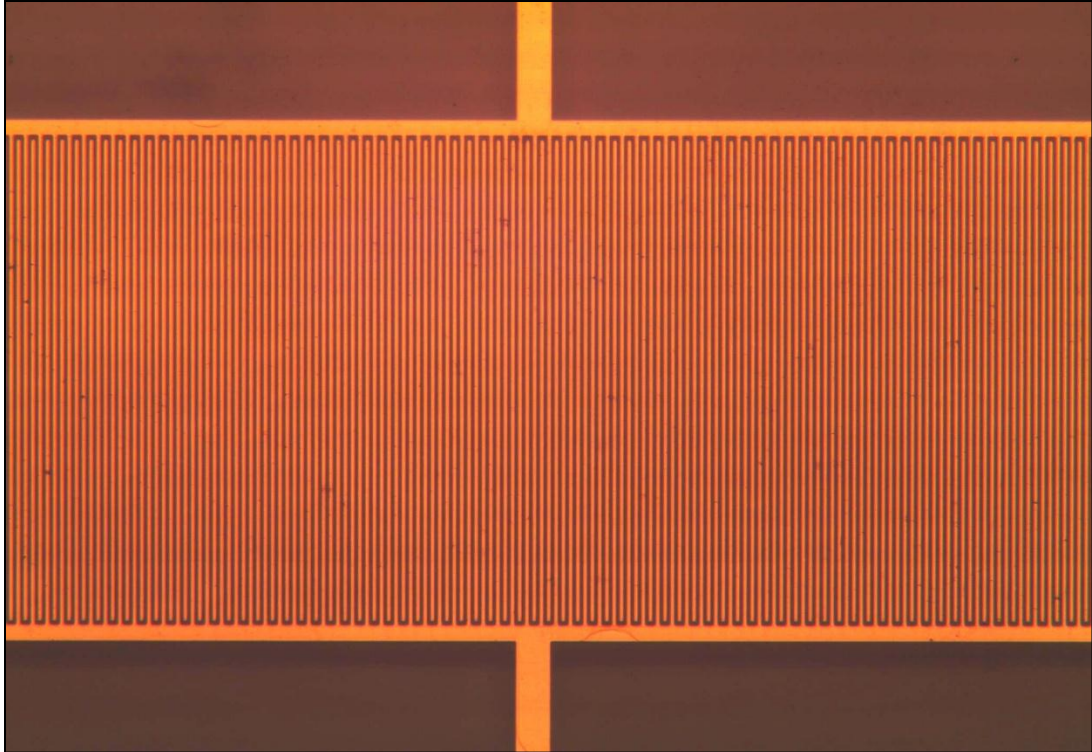


**Figure 4.7 Interdigitated Gold Microelectrodes under optical microscope**

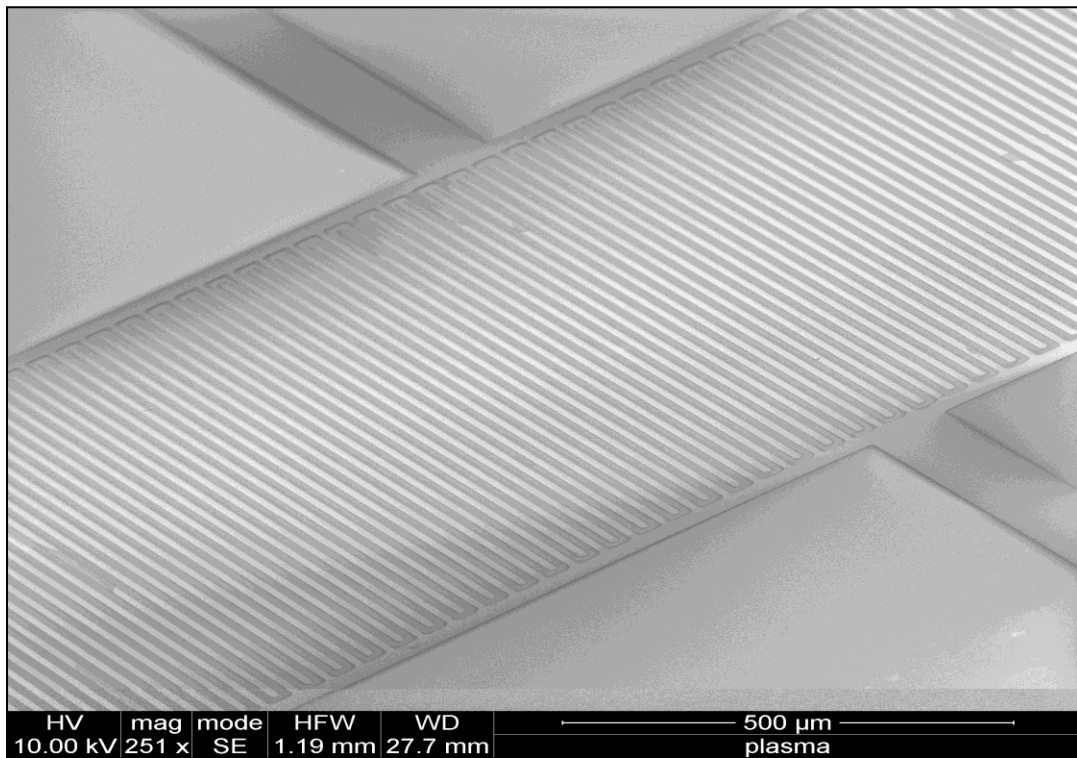


**Figure 4.8 SEM image of the Interdigitated Gold Microelectrodes**

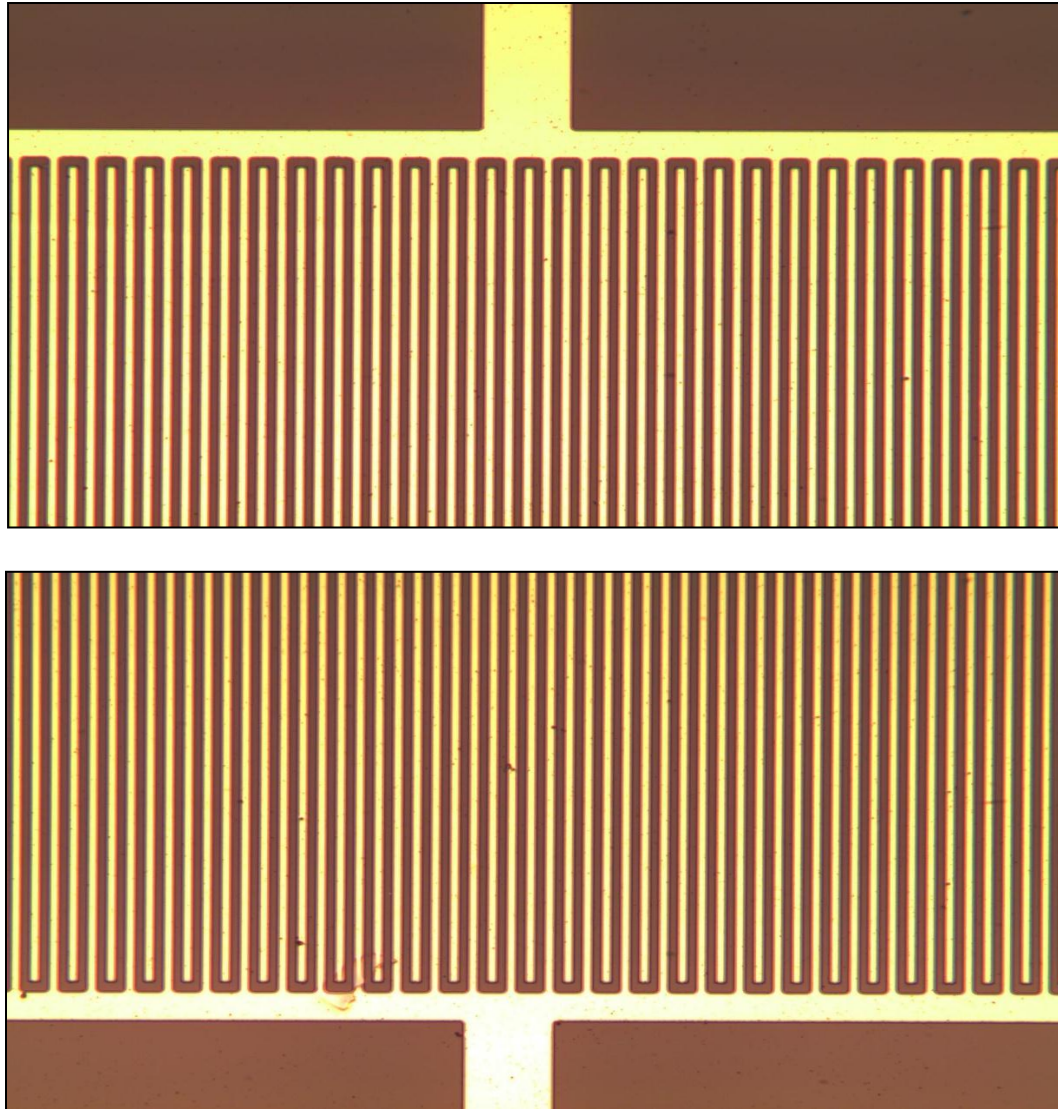


**Figure 4.9 20X Magnified view of Gold Interdigitated Microelectrodes**

#### **4.2.5 Creating PDMS Microchannel Block**

The microchannel is embedded in a PDMS slab. To create the microchannel, a master mold in shape of the microchannel is necessary. The master mold is created in SU-8 (a negative photoresist layer) on a Si substrate, using photolithography and micromachining techniques (Figure 4.10 and Figure 4.11). PDMS is obtained by mixing Sylgard 184 elastomeric base and Sylgard 184

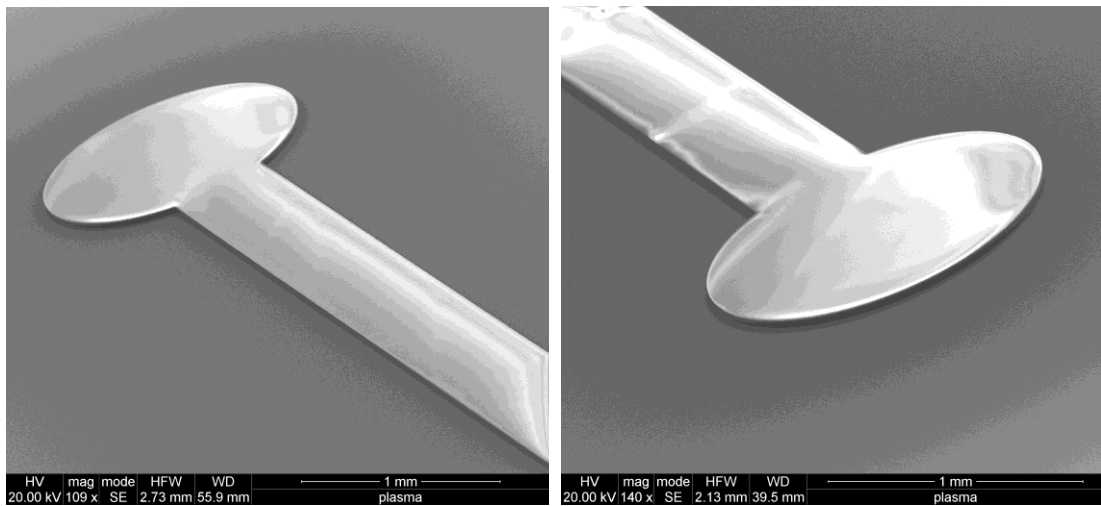
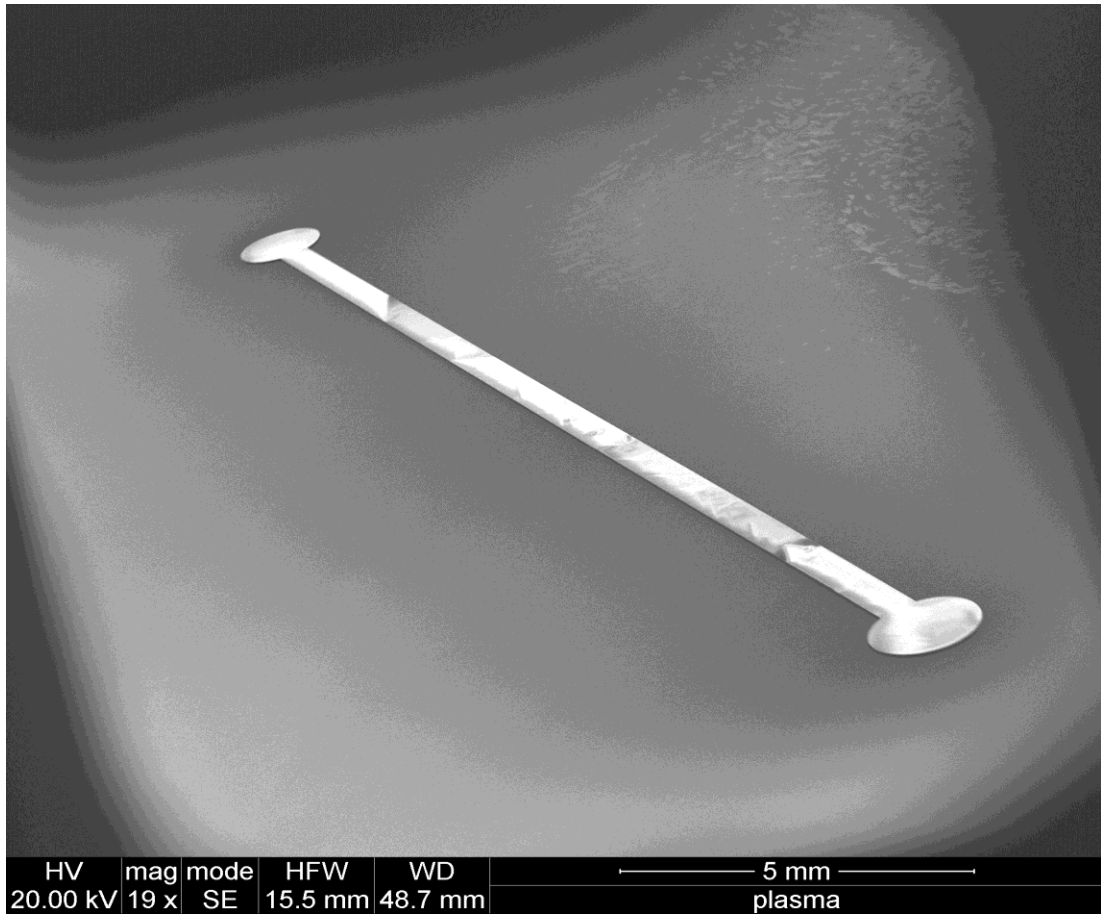


**Figure 4.10 SEM images of the Microchannel SU-8 mold on Si substrate**

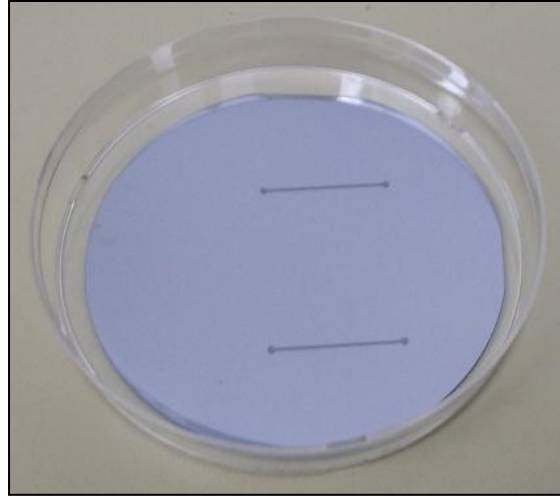


**Figure 4.11 Si substrate with SU-8 Microchannel mold**

curing agent in 10:1 ration. This mixture is poured on the master mold and cured at room temperature (25°C) for 24 hours. Once the PDMS is cured, it is peeled off from the microchannel mold (Figure 4.12). The PDMS is cut and shaped into a rectangular blocks. Finally, holes for the inlet-outlet are drilled into the PDMS. This creates the bottom layer of PDMS with microchannel embedded in it (Figure 4.12).

#### **4.2.6 Creating Top PDMS-Fluidics Connector Block**

To connect the microchannel to the fluidics connector another PDMS block with the Fluidics connectors must be created. The microfluidics connectors are glued to assume an upright position on the base of the tray and the liquid PDMS is poured into it. The PDMS is cured at room temperature (25°C) for 24 hours. Once the PDMS is cured the microfluidics connectors are strongly attached in the upright position due to the solidification of the PDMS (Figure 4.13). The PDMS is than peeled and cut into a rectangular block similar to the PDMS microchannel block.

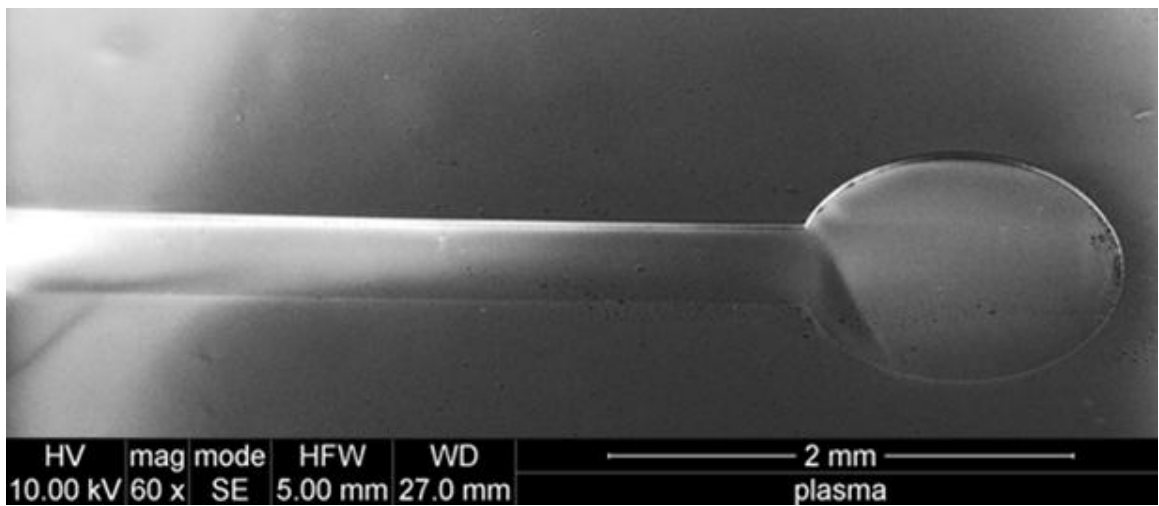
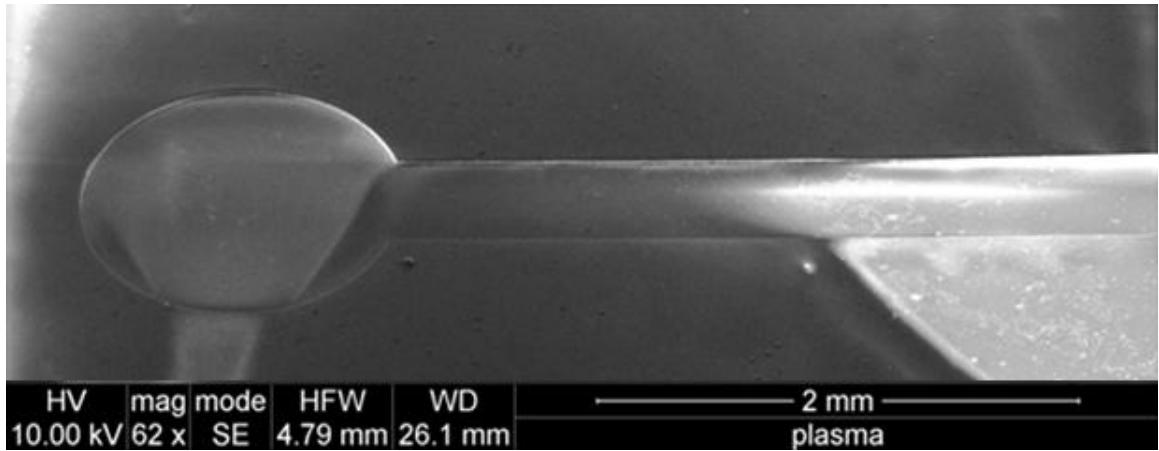


**Figure 4.12 SEM images of the inlet and outlet of the Microchannel on PDMS**

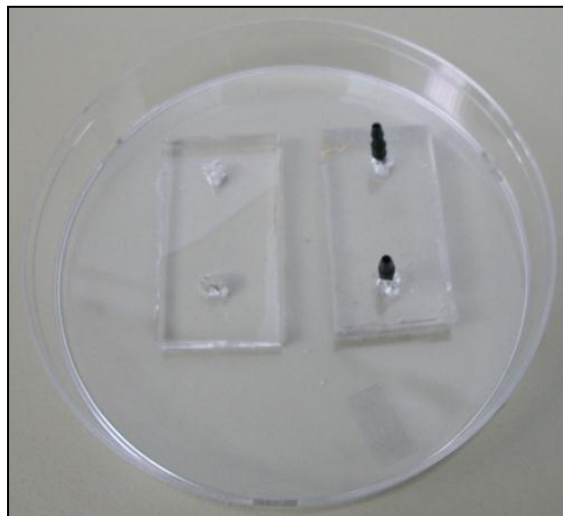


**Figure 4.13 Cured PDMS slabs with Microchannel and Microfluidics Connectors**

#### 4.2.7 Bonding PDMS to Glass

To bond the PDMS to the glass surface Oxygen Plasma treatment must be applied using Plasma Lab 800. Oxygen Plasma treatment changes the surface of the PDMS to

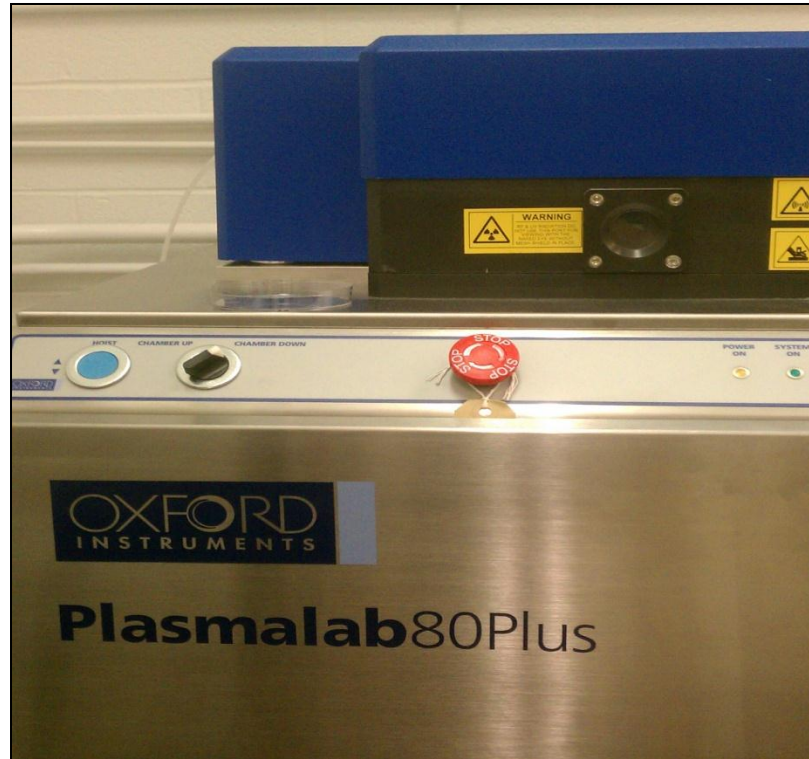


**Figure 4.14 Plasmalab 80 (Reactive Ion Etching Tool) used to bond PDMS to Glass**

hydrophilic. This helps improve the adhesion between the glass and the PDMS block.

The treated PDMS microchannel block is aligned with the interdigitated microelectrode array and pressed firmly against the glass slide. This ensures a good bonding between the glass and the PDMS block and prevents any fluid leakage. The other PDMS block is treated in similar fashion. The microfluidics connectors in this treated PDMS block are aligned with the inlet-outlet holes on the bottom PDMS layer and pressed firmly to create a good bonding between the two PDMS blocks. The fabricated device is shown in Fig.4.15



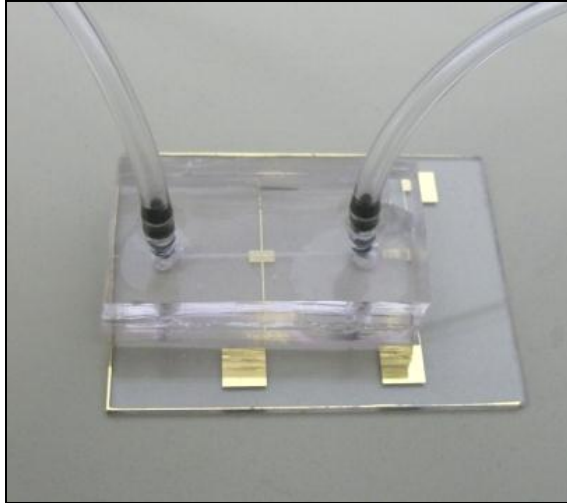


**Figure 4.15 Fabricated device**

#### **4.2.8 Wire Bonding and Packaging**

In the last step the device is attached to a PCB board. Electrical connection between the electrodes and the PCB is established through wire bonding. This step completes the fabrication of the biosensor. The packaged device is shown in fig. 4.16

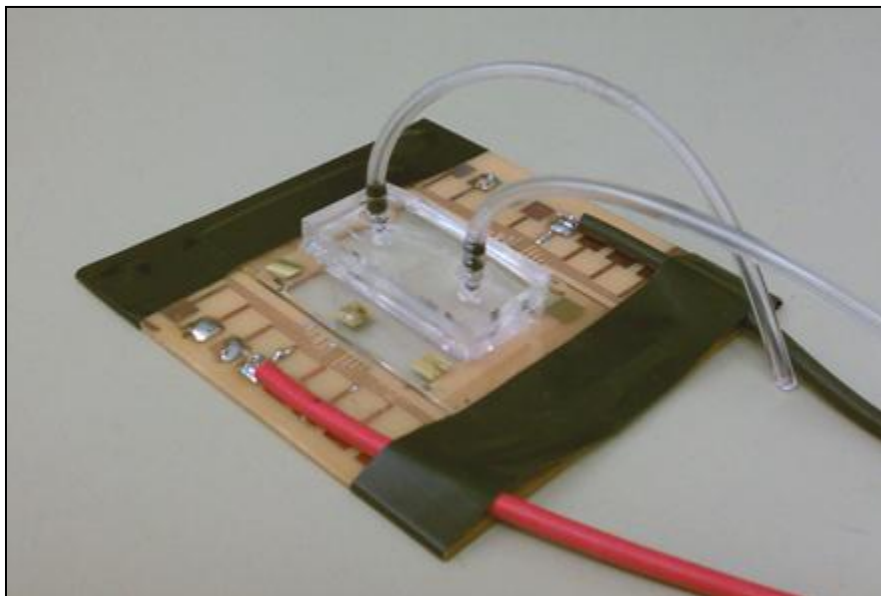


**Figure 4.16 Packaged Biosensor**

## CHAPTER 5: Test Setup and Protocol

The main purpose of a sensor is to provide a difference in output signal levels, which can be correlated to the test subjects. For the impedometric biosensor (more commonly known as the impedance biosensor), this signal corresponds to the various impedance levels when different samples are tested. By establishing a relationship between the impedance and the concentration of pathogens present in a test sample, we can characterize the functionality of the sensor.

### 5.1 Test Setup

To perform effective tests on the sensor, adequate test setup is very important. Precision test instruments are required to minimize the error and obtain good results. To perform impedance measurement for various samples with different concentrations of pathogens in it, the following instruments are used.

- Harvard PHD 4400 Syringe Pump
- Agilent 4294A Precision Impedance Analyzer
- Leica DM-IL Inverted Contrasting Microscope

The following paragraphs provide a brief description of these instruments.

### 5.1.1 Fluid Flow in the Channel

The PHD 4400 HPSI Programmable Syringe Pump, a single syringe infuse-withdraw pump is used to infuse the test samples in the microchannel of the device. A 10 ml standard syringe filled with the test sample is placed on the syringe pump and connected to the inlet of the device with tygon tube. A flow rate of  $\geq 0.5 \mu\text{m}\cdot\text{min}^{-1}$  is used to inject the test sample inside the microchannel. This optimum flow rate is chosen after several iterations. Higher flow rate fractures the microchannel and eventually results in leaking.

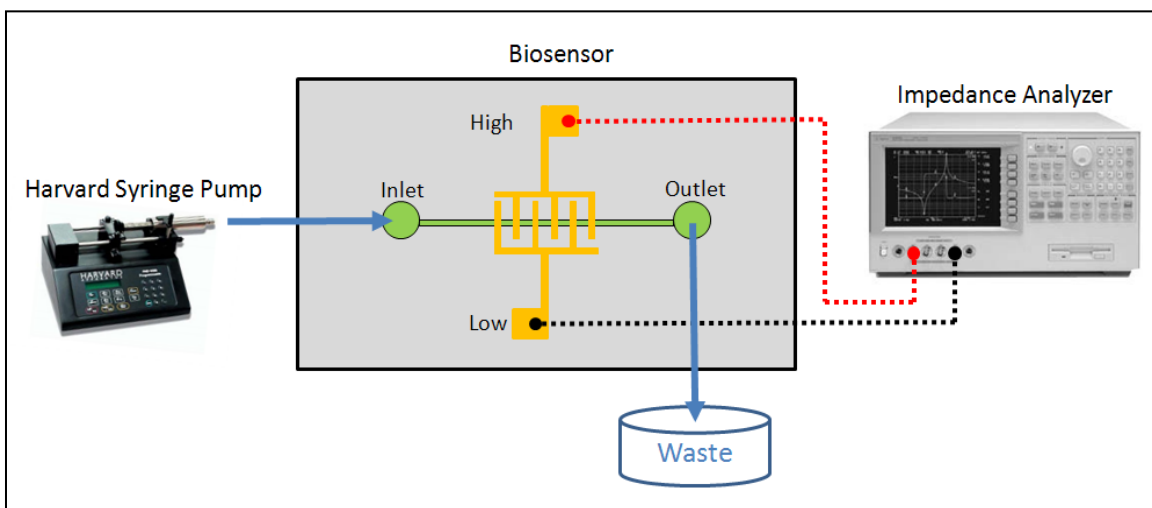


Figure 5.1 Graphical illustration of the Test setup

### 5.1.2 Agilent 4294A Precision Impedance Analyzer

To perform accurate measurement of impedance Agilent 4294A Precision Impedance analyzer is used. This impedance analyzer can measure impedance from 40Hz-110MHz frequency range. For this project we use 100Hz-1MHz frequency range to study the electrochemical phenomenon over this wide range of frequency. Measurements were performed when the microchannel was filled with test samples. The two bonding pads of the biosensor are connected to the test leads of the biosensor. A  $0.5 \text{ mV}_{\text{p-p}}$  sinusoidal signal is used as the excitation signal to perform the impedance measurement. Impedance

values were recorded for the entire frequency range and stored in the computer. Comparison graphs of different test samples were plotted at various frequency points.

### **5.1.3 Lecia DM-IL Inverted Contrasting Microscope**

To optically observe the surface of interdigitated microelectrodes the contrasting microscope was used. This microscope provides high resolution images which are recorded using software for analysis. 40X magnification was used to study the surface of the electrodes after immobilization of bacteria cells. Optical observation confirms that the change of impedance recorded by the impedance analyzer is due to the presence of bacteria cells on the electrodes.

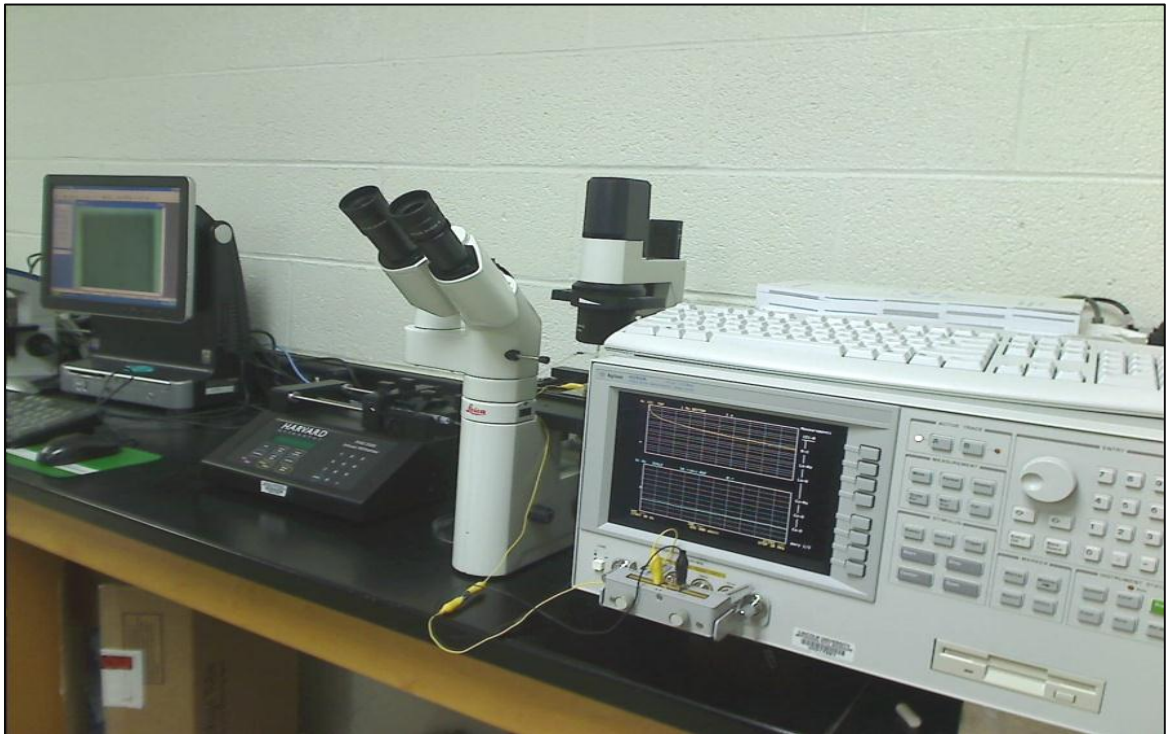


**Figure 5.2 Setup with Impedance Analyzer**

## 5.2 Chemical and Reagents

Purified goat anti-E.coli O157:H7 antibody was obtained from Biodesign International (Saco, Maine), which was used to immobilize the E.coli O157:H7 bacteria on the electrode surface. From the  $1 \text{ mg}\cdot\text{mL}^{-1}$  stock antibody solution,  $25 \text{ }\mu\text{l}$  was diluted into



**Figure 5.3 Biosensor under Microscope for Optical Observation**

$475 \text{ }\mu\text{l}$  PBS. This gave a concentration of  $50 \text{ mg}\cdot\text{mL}^{-1}$   $\alpha$ -E. coli O157:H7 antibody in 1X PBS. Phosphate Buffer Saline (PBS; 0.01 M, PH 7.4) was purchased from Sigma-Aldrich (St. Louis, MO). To wash the device and regenerate the electrode surface before each test, Hydrochloric Acid (1 miliM) was used. All the samples were tested using De-ionized (DI) water (Milli-Q,  $18.2 \text{ M}\Omega\cdot\text{cm}$ ).

### 5.3 Bacteria Culture

*E. coli* O157:H7 was ordered from American Type Culture Collection (Rockville, MD). Stock cultures of *E.coli* O157:H7 was grown for 18 to 20 hours at 37°C in Soy broth. 1 ml of contaminated soy broth was taken and was centrifuged at 1600 rcf for 10 minutes. The supernatant was removed and the cells were re-dispersed in 1 ml PBS (0.01M, pH 7.4). The re-dispersed cells were again centrifuged for 10 minutes at 1600 rcf . The supernatant was removed and the cells were re-dispersed in 10ml PBS (0.01M, pH 7.4). Four serial dilutions were prepared for testing.

1. 1 ml stock purified *E. coli* ( $3 \times 10^5$  CFU/ml)
2. 100  $\mu$ l sample (1) into 900  $\mu$ l PBS ( $3 \times 10^4$  CFU/ml)
3. 100  $\mu$ l sample (2) into 900  $\mu$ l PBS ( $3 \times 10^3$  CFU/ml)
4. 100  $\mu$ l sample (3) into 900  $\mu$ l PBS ( $3 \times 10^2$  CFU/ml)

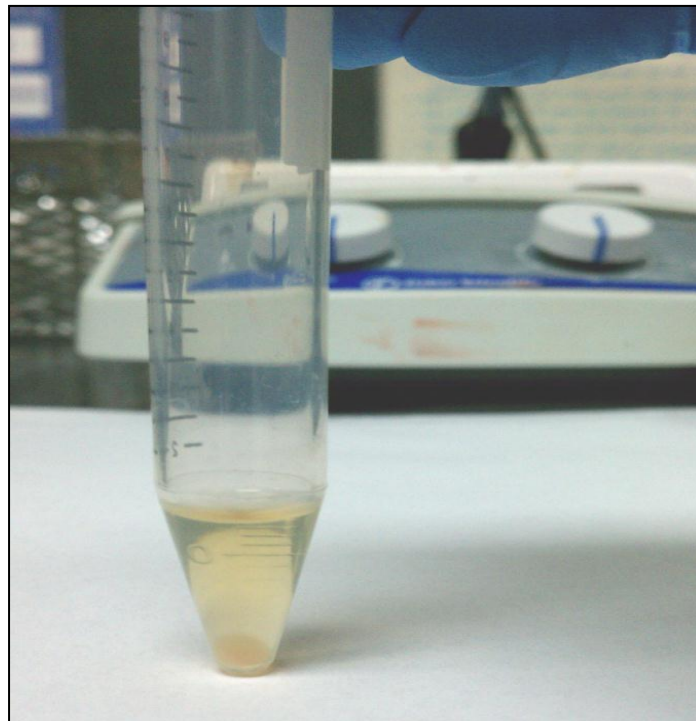


**Figure 5.4 Centrifuged Test Solution**

#### 5.4 Surface Modification and Immobilization of *E.coli* Cells

To achieve selectivity and to improve the efficiency of detection, the surface of the microelectrodes is coated with *anti-E.coli* antibody. To immobilize antibody on the electrode surface the antibody solution is sent through the inlet of the microchannel and incubated for 30 minutes at room temperature. The antibody immobilizes due to the non-specific binding to the gold electrode surface. Once the incubation period is over the electrodes are rinsed by flowing DI water in the microchannel. Rinsing the electrodes with DI water helps remove any unbound antibody from the surface of the electrodes. After successful incubation of antibody on the microelectrode array, samples with varying concentrations of *E.coli O157:H7* are tested. After each set of tests the electrode surface is cleaned using 1miliM Hydrochloric acid (HCL) solution. Modification of the electrode surface with antibody provides a good selectivity towards a particular type of cell and also assures that the response obtained from the sensor is due to the specific cell. Test samples containing various concentration of *e.coli O157:H7* bacteria were injected into microchannel through inlet. The *E.coli* cells were incubated for 30 minutes to make sure that cells have sufficient time to bind with the immobilized antibody. As the channel is filled with the *E.coli* test sample, traversing the antibody coated surface, the bacteria comes in contact with the antibody and binding takes place. After the incubation period is over the unbound bacteria, the non-specifically bound proteins and cells are removed by flushing DI water through the microchannel. The channel is filled with DI water and impedance measurement is performed from 100Hz to 1 MHz frequency. The entire process is graphically illustrated in Figure 5.4.

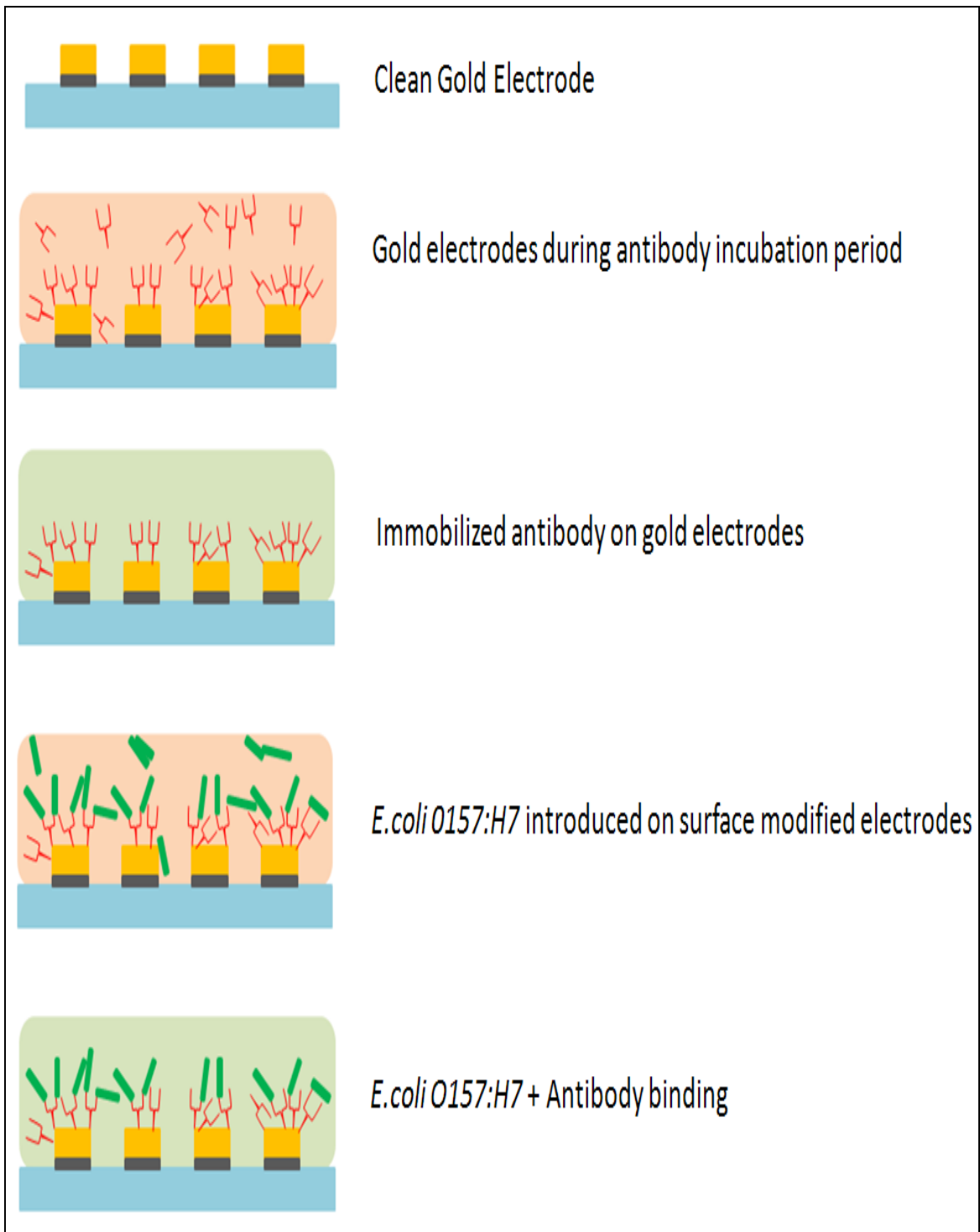


**Figure 5.5 Immobilization Process**



## CHAPTER 6: Results and Discussion

In this chapter obtained results from various experiments and tests have been presented and analyzed. The biosensor was tested with several samples and impedance responses to those samples were recorded using the impedance analyzer. The recorded impedance values were plotted using Bode Plot. The impedance comparison between different samples was also performed and plotted for various frequency points.

### 6.1 Impedance Measurement and Analysis

To understand the behavior of the biosensor, impedance response of different samples were studied. The surface of interdigitated electrodes is modified with anti-*E.coli* antibody prior to the testing. These surface modified electrodes are then tested with four concentrations of *E.coli* bacteria in three different test medium. Table 6.1 shows the four concentrations of *E. coli O157:H7* and three test mediums used for testing.

**Table 6-1 Shows the various concentrations and the test medium used for impedance measurement**

Concentration of <i>E. coli O157:H7</i>	Test sample (Medium)
$3 \times 10^5$ CFU/ml	Grape
$3 \times 10^4$ CFU/ml	Spinach
$3 \times 10^3$ CFU/ml	Turkey
$3 \times 10^2$ CFU/ml	

When the *E.coli* cells are recognized by the antibody, antibody-antigen binding occurs and this leads to a change in the dielectric property. This change was measured using impedance analyzer (Figure 6.1) over a frequency range of 100Hz to 1MHz. The impedance analyzer measures the impedance of the biosensor system. As various concentrations of bacteria are introduced the impedance changes. This change in

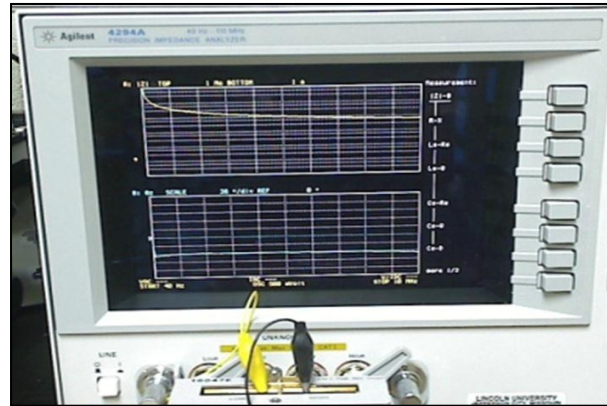


**Figure 6.1 Impedance Spectroscopy using Impedance Analyzer**

impedance is directly proportional to the amount of bacteria that binds with the antibody. After every set of testing, the electrode surface would get contaminated and become unusable. To remove the contamination and prepare a test using a new set of samples, the electrode surface is rinsed thoroughly with 1mM HCL acid solution. This process also helps in the regeneration of the electrodes. After the regeneration the electrode surface is re-modified with antibody.

## **6.2 Sensitivity Measurement**

The efficiency and utility of a sensor can be determined by its sensitivity towards the test object. The sensitivity of the interdigitated microelectrode based biosensor in detecting *E.coli* bacteria cells was studied using impedance spectroscopy. Figure 6.2 shows the

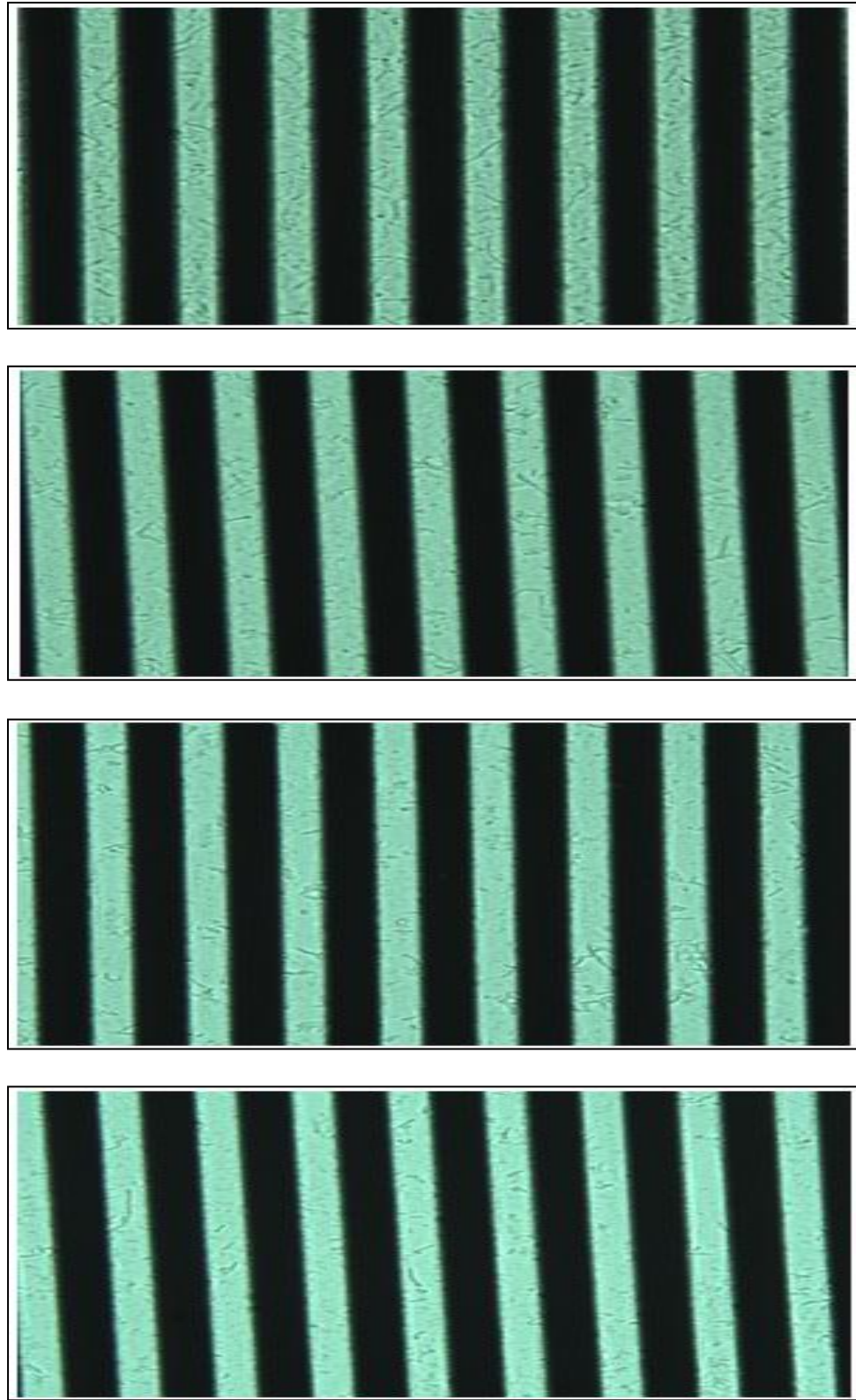


Figure 6.2 Magnified view of four concentrations of *E. coli* O157:H7 cells on Interdigitated electrodes

*E.coli O157:H7* cells of four different concentrations immobilized on the gold electrodes. The impedance response of the biosensor towards the 4 different concentrations of *E.coli* cells in a grape sample is shown in Figure 6.2. Figure 6.2(a) shows the impedance response using Bode plot and Figure 6.2(b) shows the comparison of impedance response of the four concentrations at nine different frequency points from 100Hz to 1MHz.

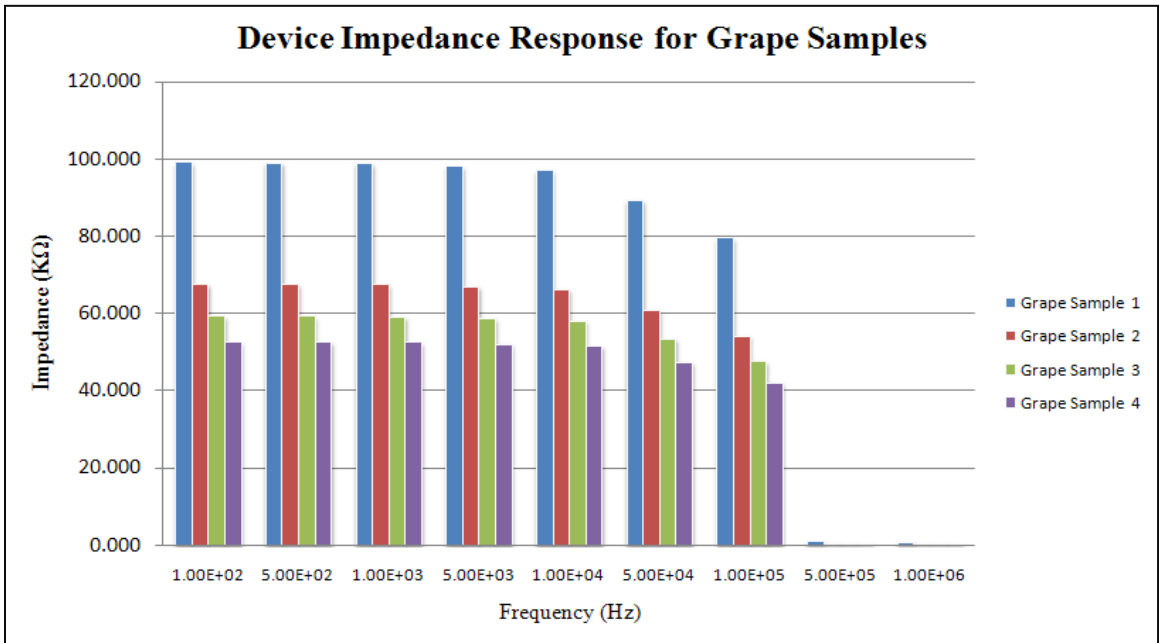
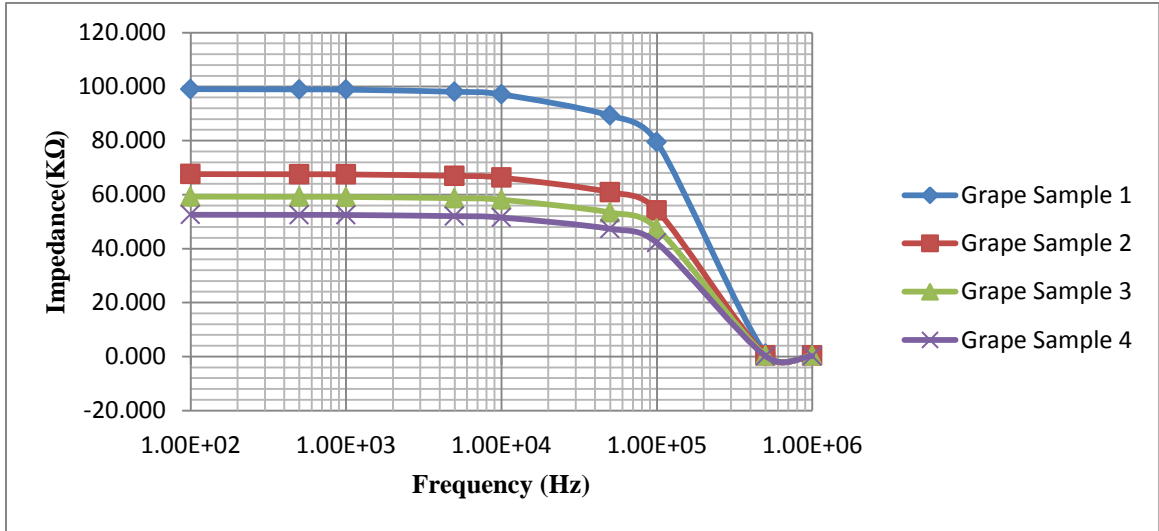


Figure 6.3 Impedance responses of four different concentrations of *E.coli O157:H7* in Grape sample

From the responses we see that the impedance not only depends on the concentration of the bacteria but also depends on the frequency. Figure 6.3 and Figure 6.4 shows the impedance response of the four concentrations of *E.coli* cells in Spinach and Turkey samples.

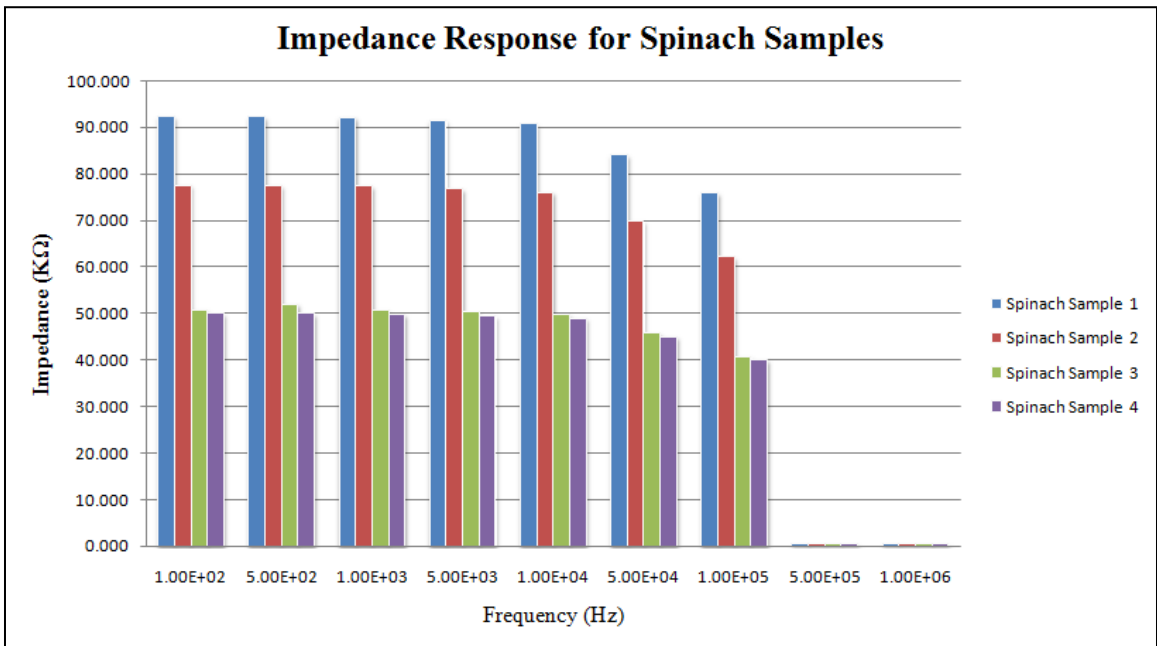
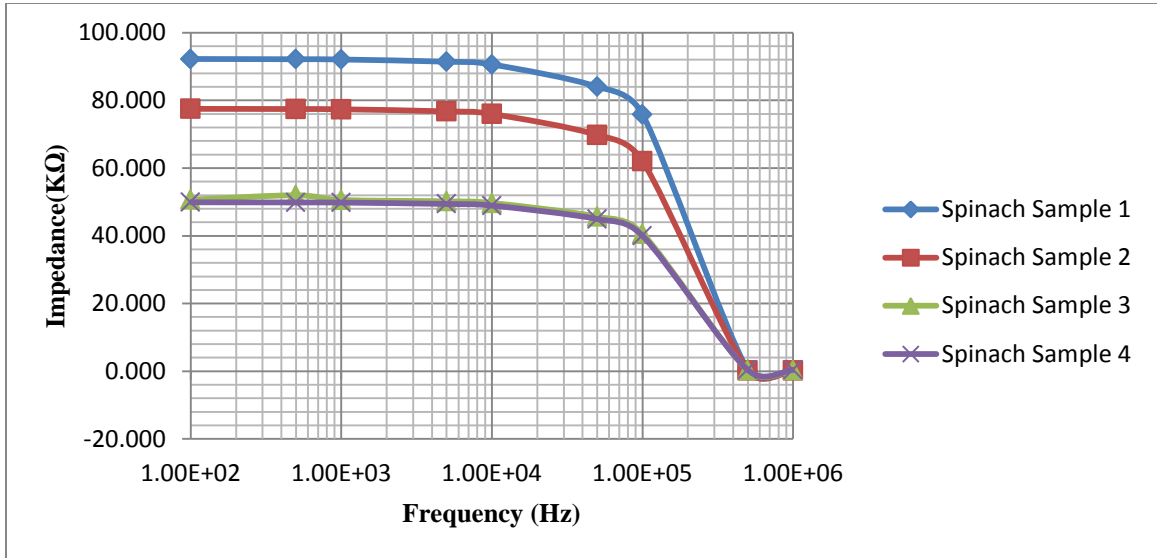
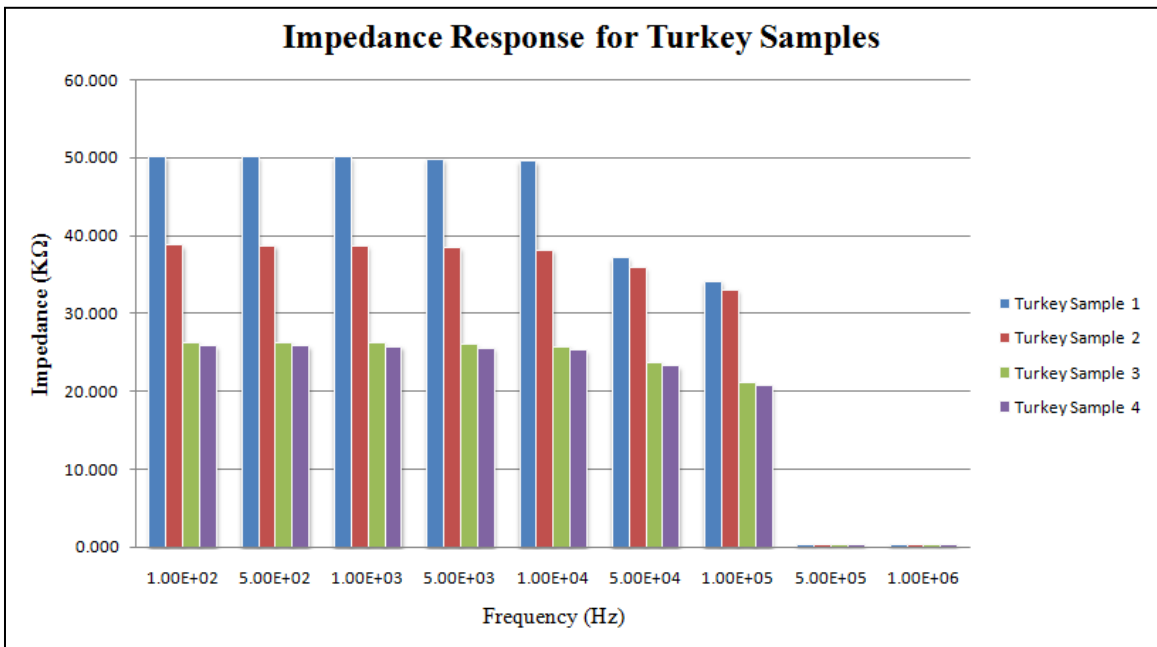
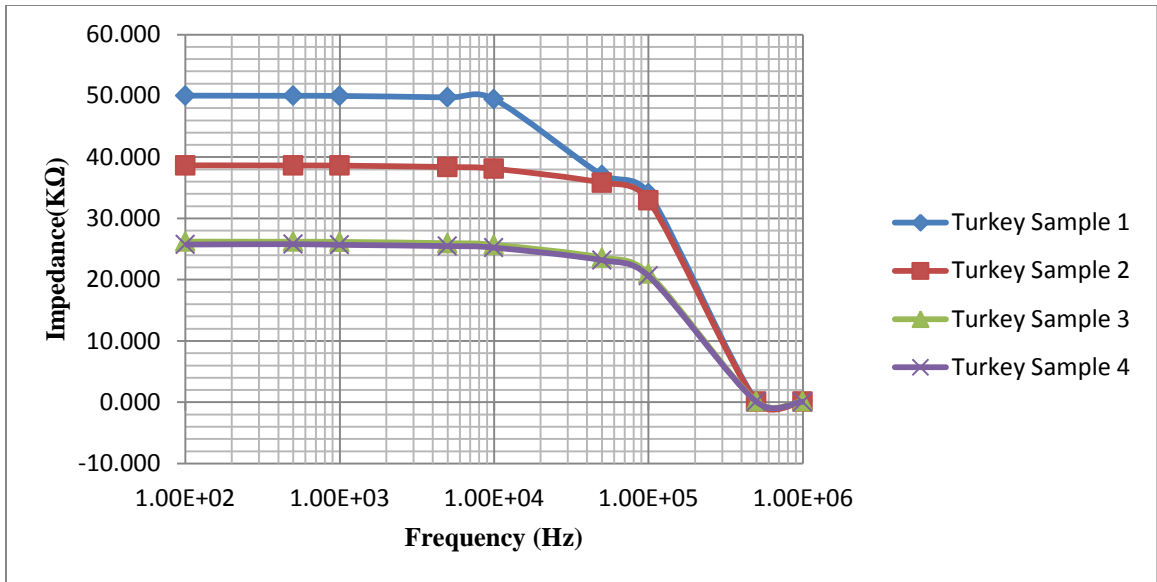


Figure 6.4 Impedance responses of four different concentrations of *E.coli* O157:H7 in Spinach sample



**Figure 6.5 Impedance responses of four different concentrations of *E.coli O157:H7* in Turkey sample**

From the response we can see that at higher frequencies ( $\geq 500$  KHz) the impedance values are very low. This is due to the fact that at higher frequencies the impedance is largely dominated by the dielectric capacitance ( $C_{de}$ ). Also at high frequencies the impedance resulting from double layer capacitance ( $C_{dl}$ ) is minimized. Higher frequencies

cause the contribution of bacteria cells to the impedance to reduce, and response becomes dependent on the dielectric properties of small dipole like bubbles and the resistance of the test sample. Thus the impedance response is very low at frequencies higher than 500 KHz. On the other hand, at lower frequencies the impedance response is more significant and the response of various samples can be easily differentiated from each other. From the analysis of the obtained data it can be seen that the impedance increases with the amount of bacteria present in the test sample. Thus we can say that at low frequencies the impedance response of the biosensor is linearly proportional to the amount of bacteria immobilized on the electrodes. This trend can be seen in all samples in the three different mediums (Figure 6.3 and Figure 6.4)

Another interesting phenomenon which can occur happens when samples with lower concentrations ( $\geq 3 \times 10^3$  CFU/ml) generate almost identical impedance response to samples with  $3 \times 10^3$  CFU/ml concentrations. This may be due to the fact that the polarization effect of the bacteria on the electrode surface only begins to impact the impedance at concentrations greater than  $3 \times 10^3$  CFU/ml. Another reason is samples with low bacteria concentration ( $>10^3$  CFU/ml) results in fewer bacteria getting immobilized on the sensor surface compared to samples with higher cell concentrations which cover significant amount of electrode surface. If only a few cells bind on to the electrode surface the change in the dielectric property due to immobilization is negligible. This results in an almost similar impedance response for concentrations lower than  $3 \times 10^3$  CFU/ml. From this study we can infer that the lowest detection limit of this interdigitated microelectrode based biosensor for *E.coli O157:H7* is  $3 \times 10^3$  CFU/mL or 3cell/ $\mu$ l.

**Table 6-2 Impedance values of four samples at nine frequency points from 100Hz to 1GHz**

<b>Frequency (Hz)</b>	<b>Grape Sample 1 (KΩ)</b>	<b>Grape Sample 2 (KΩ)</b>	<b>Grape Sample 3 (KΩ)</b>	<b>Grape Sample 4 (KΩ)</b>
1.00E+02	99.039	67.588	59.240	52.537
5.00E+02	98.961	67.534	59.193	52.496
1.00E+03	98.863	67.467	59.134	52.443
5.00E+03	98.078	66.929	58.663	52.024
1.00E+04	97.097	66.257	58.075	51.501
5.00E+04	89.250	60.881	53.371	47.311
1.00E+05	79.442	54.161	47.490	42.075
5.00E+05	0.974	0.445	0.397	0.185
1.00E+06	0.690	0.374	0.365	0.167

**Table 6-3 Impedance values of four samples at nine frequency points from 100Hz to 1GHz**

<b>Frequency (Hz)</b>	<b>Spinach Sample 1(KΩ)</b>	<b>Spinach Sample 2(KΩ)</b>	<b>Spinach Sample 3(KΩ)</b>	<b>Spinach Sample 4(KΩ)</b>
1.00E+02	92.205	77.492	50.665	49.891
5.00E+02	92.140	77.430	51.959	49.851
1.00E+03	92.058	77.353	50.575	49.802
5.00E+03	91.403	76.735	50.172	49.406
1.00E+04	90.584	75.962	49.668	48.911
5.00E+04	84.032	69.782	45.637	44.951
1.00E+05	75.843	62.057	40.599	40.001
5.00E+05	0.328	0.256	0.290	0.401
1.00E+06	0.294	0.232	0.272	0.385

**Table 6-4 Impedance values of four samples at nine frequency points from 100Hz to 1GHz**

<b>Frequency (Hz)</b>	<b>Turkey Sample 1(KΩ)</b>	<b>Turkey Sample 2(KΩ)</b>	<b>Turkey Sample 3(KΩ)</b>	<b>Turkey Sample 4(KΩ)</b>
1.00E+02	50.039	38.668	26.215	25.733
5.00E+02	50.015	38.643	26.194	25.798
1.00E+03	49.985	38.616	26.168	25.687
5.00E+03	49.747	38.388	25.960	25.482
1.00E+04	49.448	38.102	25.699	25.225
5.00E+04	37.062	35.818	23.613	23.173
1.00E+05	34.078	32.962	21.007	20.607
5.00E+05	0.212	0.118	0.151	0.083
1.00E+06	0.207	0.109	0.137	0.068



### 6.3 Test of Sensitivity towards Non-*E.coli* Bacteria

Now that the sensitivity of the biosensor has been studied and analyzed, it is time to move on to the next step testing the sensitivity of the biosensor towards non-*E.coli* bacteria. To investigate this, the test utilized *Salmonella typhimurium* bacterium samples. The impedance responses for these samples are show in Figure 6.5.

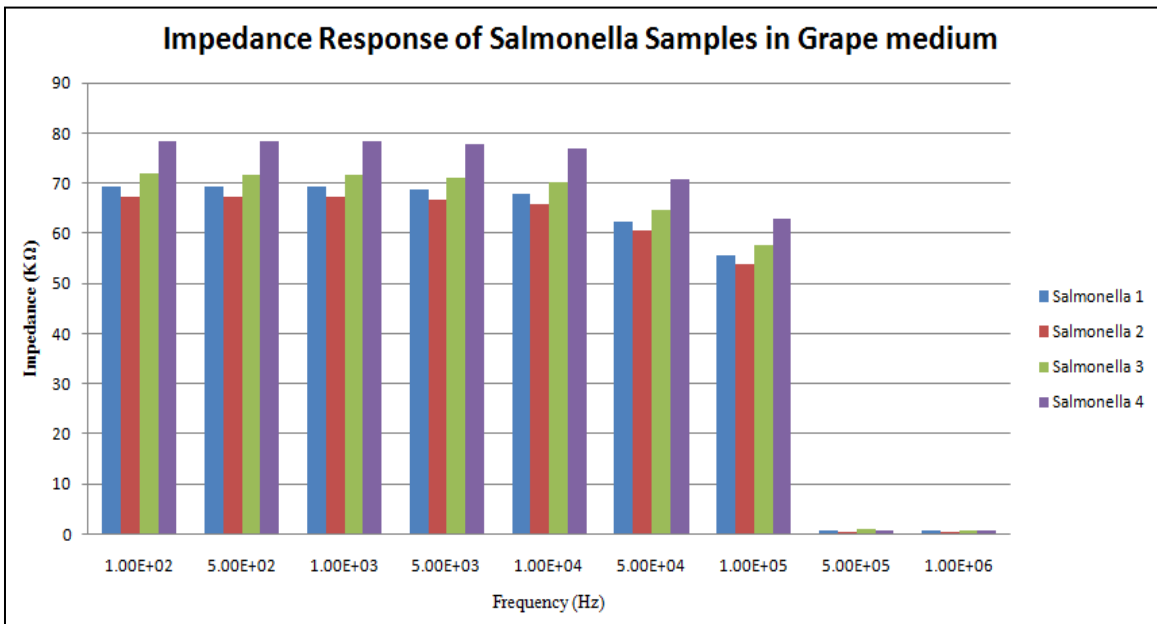
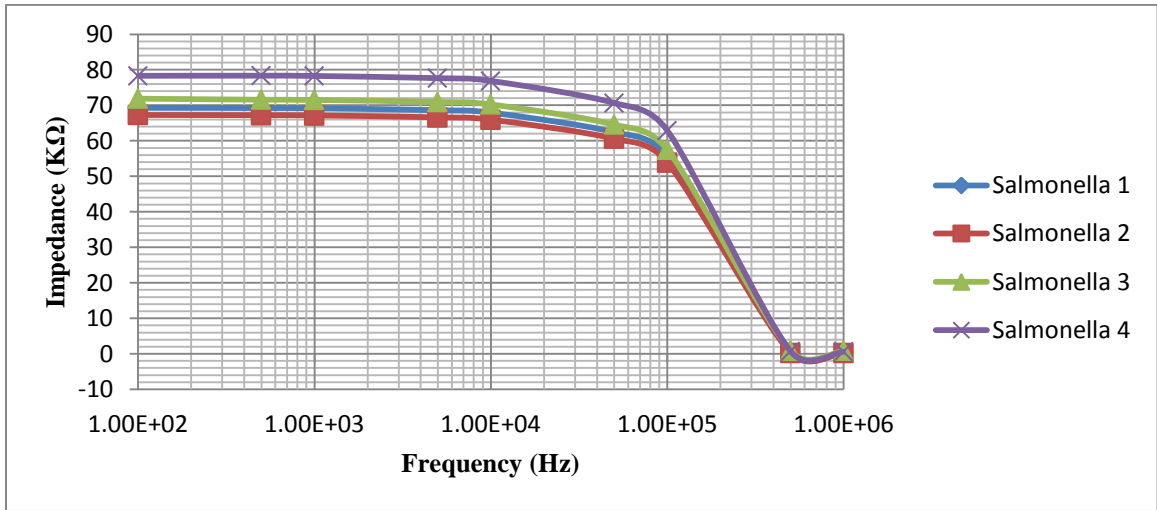


Figure 6.6 Impedance responses of *Salmonella Typhimurium* samples in Grape medium

**Table 6-5 Impedance values of four samples at nine frequency points from 100Hz to 1MHz**

<b>Frequency (Hz)</b>	<b>Salmonella 1(K<math>\Omega</math>)</b>	<b>Salmonella 2(K<math>\Omega</math>)</b>	<b>Salmonella 3(K<math>\Omega</math>)</b>	<b>Salmonella 4(K<math>\Omega</math>)</b>
1.00E+02	69.283	67.267	71.861	78.311
5.00E+02	69.228	67.213	71.574	78.338
1.00E+03	69.159	67.146	71.503	78.261
5.00E+03	68.609	66.610	70.937	77.639
1.00E+04	67.922	65.940	70.229	76.862
5.00E+04	62.425	60.580	64.551	70.644
1.00E+05	55.553	53.879	57.487	62.871
5.00E+05	0.577	0.273	0.855	0.691
1.00E+06	0.559	0.253	0.825	0.584

The same protocol was followed and the electrode surface was coated with *anti-E.coli* antibody. Four samples of *Salmonella typhimurium* with varying concentration ( $3 \times 10^5$  CFU/ml to  $3 \times 10^2$  CFU/ml, 4 serial dilutions) were prepared in grape medium and tested on the surface modified electrodes. From the impedance response of the salmonella samples we can see that the individual impedance values are in range of 67.2 K $\Omega$  to 78.3 K $\Omega$ . This happens because when *Salmonella* cells are introduced, even if they come in contact with the antibody immobilized on the gold surface, no binding takes place between *Salmonella* cells and *anti-E.coli* antibody. Although few *Salmonella* cells may still bind (non-specific binding) to the uncovered areas on the gold electrode, the change in dielectric property of the electrodes will be negligible. As the majority of the *Salmonella* cells don't bind to the electrodes, the impedance responses of the four samples are almost identical to each other. The impedance response obtained in this case is due to the double layer capacitance ( $C_{dl}$ ), resistance of the solution ( $R_{sol}$ ) and dielectric properties of small dipoles including bubbles in the test samples. This study revealed that the biosensor is not responsive to varying concentrations of *Salmonella* bacteria cells.

#### **6.4 Real-Time Measurement and Detection**

The designed interdigitated microelectrode based biosensor is realizable for everyday application and can be commercialized because it has an excellent response time. We start with a fresh device which has surface modified electrodes and connect it to the syringe pump. After flowing the test sample into the device, once the channel is filled up with the sample, we stop the syringe pump and wait 30 minutes for incubation. The impedance is continuously monitored during this period. After the incubation period we flush the device to remove cells that didn't bind and perform the impedance measurement. The total detection time using the surface modified biosensors is about 30 minutes which is very fast compared to other conventional detection techniques. The laboratory detection using Colilert/ Colitag methods (Enumeration) can take up to 24 hours [49]. The detection time of this biosensor can be reduced further by shortening the incubation period. It was observed that as the bacteria sample begins filling the biosensor device, it starts producing a measurable response within 5 minutes. So, if we reduce the incubation time to 5 minutes the total effective detection period can be reduced to 10 minutes.

## CHAPTER 7: Conclusion and Future Work

This chapter summarizes all the work related to designing, fabrication, packaging and testing of the biosensor presented in this thesis. It also discusses improvements in the design and future goals and opportunities for development.

### 7.1 MEMS Based Impedance Biosensor for *E.coli* O157:H7 Detection

*Escherichia coli* O157:H7 (*E. coli*) is a gram-negative rod-shaped bacterium. The pathogenic strain of *E.coli* bacteria can cause serious diseases like urinary tract infections, respiratory illness such as pneumonia, and other illnesses including possible diarrhea, seizure, stroke, kidney failure and even death. Every year infections caused by *E.coli* are estimated to be about 73,000 in the United States. *E. coli* can have significant impact on national and international economics due to food contamination, product recalls and medical costs. *E.coli* can often occur in vegetables, fruits, unpasteurized milk, juice, meat, and non-chlorinated water. Researchers have found that infectious doses of *E. coli* O157:H7 can be as low as 10 cells (Federal Register, 1990, 1991). Therefore, it is very important to develop effective detection techniques of *E.coli* in food products.

With this goal in mind a MEMS biosensor based on impedance spectroscopy has been developed for detection of pathogenic strain of *E.coli* O157:H.7. Two different designs

of the biosensor are presented here. The first design consists of a planar interdigitated electrode array and a microchannel. The interdigitated electrode array is called the detection array because the detection of *E.coli* takes place here. This biosensor was tested with various concentrations of *E.coli* samples in three different food products, grape, spinach and turkey meat. The presence of the *E.coli* cells is detected based on the principle of impedance spectroscopy. At first, the bacteria cells are immobilized on the surface of the interdigitated electrodes with the help of goat *anti-E.coli polyclonal IgG* antibody. This immobilization of the cells causes the dielectric property of the electrodes to change. Change in dielectric property results in a change of the biosensor's impedance and is measured with an impedance analyzer. This change in impedance can be correlated with the concentration of *E.coli* cells present in a sample.

The other proposed design of the biosensor has two sets of 3-D interdigitated electrode array and a microchannel. The first array of electrodes is called the focusing array and the second array is called the detection array. The focusing array uses dielectrophoresis to separate the unwanted objects from the *E.coli* cells which improves the efficiency of detection. As this is a 3-D design, it also increases the ratio of sensing surface to volume compared to the two-dimensional (2-D) biosensor. This increased surface-to-volume ratio enhances the resolution of the impedance spectrum and will provide better detection.

## **7.2 The Study of Sensitivity**

For any sensor, its sensitivity towards the test object is an important parameter of performance. To investigate the sensitivity of the biosensor, it has been tested with four different concentrations of *E.coli O157:H7* cells in three different food products. From

the analysis of the results it can be concluded that the designed biosensor is responsive to *E.coli* concentration of  $3 \times 10^3$  CFU/ml and above. This means it can successfully detect the presence of *E.coli O157:H7* up to 3 bacterium/ $\mu$ l. It is also seen that the biosensor operates in optimal condition in a wide range of frequencies, from 100 Hz to 100 KHz. This adds to the versatility of the biosensor.

Another important performance parameter for a sensor is its response can be limited towards certain test object(s) and hence improving the accuracy of detection. The response towards another type of bacterium cell was performed using *Salmonella typhimurium*. Four different concentrations of *Salmonella* were prepared and tested using the same protocol. From the analysis of the obtained response it was observed that impedance values for the 4 concentrations of *Salmonella* are similar. This shows that the biosensor is not responsive to *Salmonella* and hence proves its selectivity towards *E.coli O157:H7* samples.

### **7.3 Scope of Commercialization**

The developed biosensor can successfully detect *E.coli O157:H7* cells even at very low concentrations. Also the detection and response time of the biosensor is less than 30 minutes. This detection time can be further reduced to 10 minutes. But with this biosensor, the detection time is less than an hour. As this biosensor is small and portable it can also accommodate onsite testing. The selectivity of the biosensor can be altered by changing the type of antibody which is immobilized on the sensor surface and can be used for detecting other types of pathogens. All these features including optimal

sensitivity, selectivity and fast response time gives the biosensor great potential as a health risk alleviating tool for commercial and societal applications.

#### **7.4 Future Work**

The future goal is to fabricate the second design of the biosensor. This device would have response time and will be more efficient. Also the existing device will be tested with other types of harmful pathogenic bacteria (such as *Salmonella typhimurium*) by changing the recognition element (antibody). The limitation of detection at high frequencies will also be explored in future work. All these improvements will lead to a complete integration of detection and analysis in a single biosensor system.

## REFERENCES

1. J.W. Judy, "Microelectromechanical systems (MEMS): fabrication, design and applications," *Smart Mater. Struct.*, vol. 10, pp.1115–1134, 2001.
2. J. Bryzek, "Impact of MEMS technology on society" *Sensors Actuators A: Physical*, vol. 56, pp. 1–9, 1996.
3. Committee on Advanced Materials and Fabrication Methods for Microelectromechanical Systems, Commission on Engineering and Technical Systems and National Research Council, 'Microelectromechanical Systems Advanced Materials and Fabrication Methods', National Academy Press, 1997.
4. M. Mehregany and S. Roy, 'Introduction to MEMS', 2000, Microengineering Aerospace Systems, Aerospace Press, AIAA, Inc., 1999.
5. M. Madou, 'Fundamentals of Microfabrication: The Science of Miniaturization.' Second Edition, CRC Press, 2002.
6. S. S. Saliterman, "Fundamentals of BioMEMS and Medical Microdevices," *SPIE Press Monograph*, vol. PM153, 2006.
7. R. Bashir, "BioMEMS: State-of-the-Art in Detection, Opportunities and Prospects," *Advanced Drug Delivery Reviews*, vol. 56, pp 1565-1586, 2004.
8. T. Vo-Dinh, B. Cullum, "Biosensors and biochips: advances in biological and medical diagnostics", *Fresenius' J. Anal. Chem.* vol. 366, pp. 540–551, 2000.
9. L. J. Kricka, "Microchips, microarrays, biochips and nanochips: personal laboratories for the 21st century", *Clinica Chim. Acta.*, vol. 307, pp.219 - 223, 2001.
10. B. H. Weigl, R. L. Bardell and C. R. Cabrera, "Lab-On-A-Chip For Drug Development", *Adv. Drug Deliv. Rev.* 55 vol.24, pp. 349-377, 2003.
11. S.M. Radke, E.C. Alocilja, "A high density microelectrde array biosensor for detection of E.coli O157:H7," *Biosens. Bioelectron.* vol. 20, pp. 1662–1667, 2005.
12. E. Bakker, Y. Qin, "Electrochemical Sensors," *Anal. Chem.* vol. 78, pp. 3965–3983, 2006
13. A.W. Bott, *Curr. Sep.* vol. 19, pp. 71–75, 2001.



14. J. Guam, Y. Miao, Q. Zhang, "Impedimetric biosensors," *J. Biosci. Bioeng.* vol. 97, pp. 219–226, 2004.
15. L. Yang, Y. Li and G.F. Erf, "Interdigitated array microelectrode-based electrochemical impedance immunosensor for detection of Escherichia coli O157:H7," *Anal. Chem.*, vol. 76, pp. 1107-1113, 2004.
16. S.M. Radke, E.C. Alocilja, "Design and Fabrication of a Microimpedance Biosensor for Bacterial Detection," *IEEE Sensors Journal*, vol. 4, pp. 434–440, 2004.
17. L. Yang, Y. Li, "AFM and impedance spectroscopy characterization of the immobilization of antibodies on indium-tin oxide electrode through self-assembled monolayer of epoxysilane and their capture of Escherichia coli O157:H7," *Biosensors and Bioelectronics*, vol. 20, pp. 1407-1416, 2004.
18. R. Gomez, R. Bashir, A. Sarikaya, M.R. Ladisch, J. Sturgis, J.P. Robinson, T. Geng, A.K. Bhunia, H.A. Apple and S. Wereley, "Microfluidic biochip for impedance spectroscopy of biological species," *Biomed. Microdev.*, vol. 3, pp. 201–209, 2001.
19. R. Gomez-Sjöberg, T. Morisette and R. Bashir, "Impedance microbiology-on-a-chip: Microfluidic bioprocessor for rapid detection of bacterial metabolism," *J. Microelectromech. Syst.*, vol.14, pp. 829–838, 2005.
20. L. Yang, Y. Li, "Detection of viable Salmonella using microelectrode-based capacitance measurement coupled with immunomagnetic separation," *J. Microbiol. Method*, vol. 64, pp. 9–16, 2006.
21. M. Varshney, Y. Li, "Interdigitated array microelectrode based impedance biosensor coupled with magnetic nanoparticle-antibody conjugates for detection of Escherichia coli O157:H7 in food samples," *Biosens. Bioelectron.*, vol. 22, pp. 2408–2414, 2007.
22. M. Varshney, Y. Li, B. Srinivasan, S. Tung, "A label-free, microfluidics and interdigitated array microelectrode-based impedance biosensor in combination with nanoparticles immunoseparation for detection of Escherichia coli O157:H7 in food samples," *Sens. Actuators B: Chem.*, vol. 128, pp. 99–107, 2007.
23. H. Li, R. Bashir, "Dielectrophoretic separation and manipulation of live and heat-treated cells of Listeria on microfabricated devices with interdigitated electrodes," *Sens. Actuators B: Chem.*, pp. 86, 215–221, 2002.

24. J. Suehiro, R. Yatsunami, R. Hamada and M. Hara, "Quantitative estimation of biological cell concentration suspended in aqueous medium by using dielectrophoretic impedance measurement method," *J. Appl. Phys.*, vol.32, pp. 2814–2820, 1999.
25. J. Suehiro, D. Noutomi, R. Hamada and M. Hara, *Proc. IEEE. 36th Ann. Meet. Indust. Appl. Soc.*, pp. 1950-1955, 2001.
26. J. Suehiro, M. Shutou, T. Hatano, M. Hara, "High sensitive detection of biological cells using dielectrophoretic impedance measurement method combined with electropermeabilization," *Sens. Actuators B: Chem.*, vol. 96, pp. 144–151, 2003.
27. F. Aldaeus, Y. Lin, J. Roeraade and J. Amberg, "Superpositioned dielectrophoresis for enhanced trapping efficiency," *Electrophoresis*, vol. 26, pp. 4252–4259, 2005.
28. W. Laureyn, D. Nelis, P. Van Gerwen, K. Baert, L. Hermans, R. Magnee, J.J. Pireaux, and G. Maes, "Nanoscaled interdigitated titanium electrodes for impedimetric biosensing," *Sens. Actuators B: Chem.*, vol. 68, pp. 360–370, 2000.
29. C. Ruan, L. Yang, Y. Li, "Immunosensor chips for detection of *E. coli* O157:H7 using electrochemical impedance spectroscopy," *Anal. Chem.*, vol.74, pp. 4814–4820, 2002.
30. S.K. Kim, P.J. Hesketh, C. Li, J.H. Thomas, H.B. Halsall, and W.R. Heineman, "Fabrication of comb interdigitated electrodes array(IDA) for a microbead-based electrochemical assay system," *Biosens. Bioelectron.*, vol.20, pp. 887–894, 2004.
31. J.H. Thomas, S.K. Kim, P.J. Hesketh, H.B. Halsall, and W.R. Heineman, "Microbead-based electrochemical immunoassay with interdigitated array electrodes," *Anal. Biochem.* vol.328, pp. 113–122, 2004.
32. B.C. Towe, V.B. Pizziconi, "A microflow amperometric glucose biosensor," *Biosens. Bioelectron.* vol.12, pp. 893–899, 1997.
33. C. Berggren, B. Bjarnason and G. Johansson, "An immunological interleukine-6 capacitive biosensor using perturbation with a potentiostatic step," *Biosens. Bioelectron.* vol.13, pp. 1061–1068, 1998.
34. V.M. Mirsky, M. Mass, C. Krause and O.S. Wolfbeis, "Capacitive Approach to Determine Phospholipase A2 Activity toward Artificial and Natural Substrates," *Anal. Chem.* vol.70, pp. 3674–3678, 2004.

35. M. Varshney, Y. Li, "Interdigitated array microelectrodes based impedance biosensors for detection of bacterial cells," *Biosensors and Bioelectronics*, vol.24, pp. 2951–2960, 2009.
36. M. Ciszowska, Z. Stojek, "Voltammetry in solutions of low ionic strength. Electrochemical and analytical aspects," *J. Electroanal. Chem.*, vol. 466, pp. 129–143, 1999.
37. C. Amatore, J.M. Saveant, and D. Tessier, "Kinetics of electron transfer to organic molecules at solid electrodes in organic media" *J. Electroanal. Chem. Interface Electrochem.* vol.146, pp. 37–45, 1983.
38. K. Mauyama, H. Ohkawa, S. Ogawa, A. Ueda, O. Niwa, and K. Suzuki, "Fabrication and characterization of a nanometer-sized optical fiber electrode based on selective chemical etching for scanning electrochemical/optical microscopy," *Anal. Chem.* vol.78, pp. 1904–1912, 2006.
39. Y. Liu, T.M. Walter, W. Chang, K. Lim, L. Yang, S.W. Lee, A. Aronson, and R. Bashir, "Electrical detection of germination of viable model *Bacillus anthracis* spores in microfluidic biochips," *Lab Chip*, vol.7, pp. 603–610, 2007.
40. E. Nebling, T. Grunwald, J. Albers, P. Schafer, R. Hintsche, "Electrical detection of viral DNA using ultramicroelectrode arrays," *Anal. Chem.*, vol.76, pp. 689–696, 2004.
41. G. Kim, M. Morgan, B. K. Hahm, A. Bhunia, J. H. Mun, and A. S. Om, "Interdigitated microelectrode based impedance biosensor for detection of salmonella enteritidis in food samples," *J. Phys.: Conf. Ser.* vol.100, 2008
42. B. B. Narakathu, B. E. Bejcek, and M. Z. Atashbar, "Impedance based Electrochemical Biosensors," *IEEE Sensors* pp. 1212-1216, 2009.
43. K.R. Foster, H.P. Schwan, "Dielectric properties of tissues and biological materials: a critical review," *Crit. Rev. Biomed. Eng.* vol.17 pp. 25–104, 1989.
44. A. Minerick, R. Pethig, "Dielectrophoresis," The American electrophoresis Society <http://www.aesociety.org/areas/dielectrophoresis.php>
45. C. Zhang, K. Khoshmanesh, A. Mitchell, and K. Kalantar-zadeh "Dielectrophoresis for manipulation of micro/nano particles in microfluidic systems," *Anal. Bioanal. Chem.*, vol.396 pp. 401–420, 2010.
46. L. Guzman, A. Miotello, R. Checchetto, and M. Adami, "Ion beam-induced enhanced adhesion of gold films deposited on glass," *Surf. Coat. Tech.*, vol. 158-159, pp. 558-562, 2002

47. A. Folch, A. Ayon, O. Hurtado, M. A. Schmidt, and M. Toner, "Molding of Deep Polydimethylsiloxane Microstructures for Microfluidics and Biological Applications," *J. Biomech. Engg.*, vol. 121, pp. 28-34, 1999.
48. K.S. Yun, E. Yoonb, "Fabrication of complex multilevel microchannels in PDMS by using three-dimensional photoresist masters," *Lab Chip 2008*, vol.8, pp 245–250, 2008.
49. MACS Lab "E. Coli/Bacteria Analysis" <http://www.macslab.com/ecoli.html>